by the amounts of peroxides generated (Fig. 2). These findings suggest that olmesartan, at a clinical concentration, protects HSA against the general oxidation caused by hydroxyl radicals. In fact, olmesartan is a biphenyl tetrazole derivative and its common core structure, 5-(4′-methylbiphenyl-2-yl)-1H-tetrazol, is thus probably responsible for the inhibitory effect on oxidative stress (*15*). This structure is also important for binding to AT1 receptors and is one of the active sites of the inverse agonist. Furthermore, the imidazole ring of olmesartan has carboxyl and hydroxyl groups different from those in other ARBs, which may be the reason for its potent inverse agonist activity.

The findings of our *in vivo* study clearly demonstrated that olmesartan caused a decrease in the levels of oxidized albumin in HD patients after 4 weeks of treatment and this effect was maintained until 8 weeks (Fig. 4), while olmesartan therapy significantly reduced SBP and DBP at 8 weeks (data not shown). Therefore, these results suggest that olmesartan not only reduces SBP but also reduces oxidative stress. Angiotensin II plays an important role in increasing BP by stimulating AT1 receptors. To prevent angiotensin II from acting, ARBs block the binding of angiotensin II to AT1 receptors. Since ARBs block the effects of angiotensin II, they might be expected to decrease the risk of coronary artery disease, cardiac failure, renal dysfunction, and cerebral artery diseases (*38*). Some studies have shown that ARBs do, in fact, significantly reduce these risks, and that their mechanisms of action may involve the blocking of angiotensin II–related functions, such as inducing the production of growth factors and cytokines, in addition to their hypotensive effect. Moreover, angiotensin II has been reported to modulate NADPH oxidase activity in a number of studies, and aldosterone has also been implicated in the generation of reactive oxygen species (*7*, *39*, 40). In theory, then, blocking of the RAAS by ARBs should be effective for reducing oxidative stress. In this work, we showed that olmesartan exhibited antioxidant activity *in vivo*, but this activity might have been a combination of direct and indirect antioxidant effects, such as modulation of NADPH oxidase activity. Moreover, various factors in addition to the above effects may play a role in the antioxidant activity of olmesartan. Therefore, determining the mechanism by which olmesartan decreases the ROS production will require further *in vitro* and *in vivo* studies.

We recently demonstrated that telmisartan effectively lowered the extent of BP and reduced oxidative stress and that it is safe and well-tolerated by HD patients (*17*). Interestingly, the reduction of oxidative stress by olmesartan was slightly higher than that by telmisartan. This effect might have been due to its structure and strong binding to AT1 receptors. However, a long-term study in a large population is required to elucidate the influence of olmesartan therapy on CVD mortality and morbidity in HD patients.

In summary, olmesartan effectively lowered the extent of oxidative damage to HSA in *in vitro* and *in vivo* studies, and this effect might confer benefits beyond simple BP reduction.

## Acknowledgements

We wish to thank the Sankyo Pharmaceutical (Tokyo, Japan) for the generous gift of olmesartan.

## References

1. Suzuki H: Treatment of hypertension in chronic renal insufficiency. *Intern Med* 2000; **39**: 773–777.
2. Suzuki H: Angiotensin type 1 receptor blockers in chronic kidney disease. *Contrib Nephrol* 2004; **143**: 159–166.
3. Okada K, Hirano T, Ran J, Adachi M: Olmesartan medoxomil, an angiotensin II receptor blocker ameliorates insulin resistance and decreases triglyceride production in fructose-fed rats. *Hypertens Res* 2004; **27**: 293–299.
4. Mizuno M, Sada T, Kato M, Koike H: Renoprotective effects of blockade of angiotensin II AT1 receptors in an animal model of type 2 diabetes. *Hypertens Res* 2002; **25**: 271–278.
5. Martina B, Dieterle T, Sigle JP, Surber C, Battegay E: Effects of telmisartan and losartan on left ventricular mass in mild-to-moderate hypertension. A randomized, double-blind trial. *Cardiology* 2003; **99**: 169–170.
6. Koh KK, Ahn JY, Han SH, *et al*: Pleiotropic effects of angiotensin II receptor blocker in hypertensive patients. *J Am Coll Cardiol* 2003; **42**: 905–910.
7. Griendling KK, Minieri CA, Ollerenshaw JD, Alexander RW: Angiotensin II stimulates NADH and NADPH oxidase activity in cultured vascular smooth muscle cells. *Circ Res* 1994; **74**: 1141–1148.
8. Ruiz-Ortega M, Lorenzo O, Ruperez M, Konig S, Wittig B, Egido J: Angiotensin II activates nuclear transcription factor κB through AT1 and AT2 in vascular smooth muscle cells: molecular mechanisms. *Circ Res* 2000; **86**: 1266–1272.
9. Tschudi MR, Mesaros S, Luscher TF, Malinski T: Direct *in situ* measurement of nitric oxide in mesenteric resistance arteries: increased decomposition by superoxide in hypertension. *Hypertension* 1996; **27**: 32–35.
10. Weiss D, Kools JJ, Taylor WR: Angiotensin II–induced hypertension accelerates the development of atherosclerosis in ApoE-deficient mice. *Circulation* 2001; **103**: 448–454.
11. Haller H, Viberti GC, Mimran A, *et al*: Preventing microalbuminuria in patients with diabetes: rationale and design of the Randomised Olmesartan and Diabetes Microalbuminuria Prevention (ROADMAP) study. *J Hypertens* 2006; **24**: 403–408.
12. Yamaguchi K, Ura N, Murakami H, *et al*: Olmesartan ameliorates insulin sensitivity by modulating tumor necrosis factor-alpha and cyclic AMP in skeletal muscle. *Hypertens Res* 2005; **28**: 773–778.
13. Izuhara Y, Nangaku M, Inagi R, *et al*: Renoprotective properties of angiotensin receptor blockers beyond blood pressure lowering. *J Am Soc Nephrol* 2005; **16**: 3631–3641.
14. Yuan Z, Nimata M, Okabe TA, *et al*: Olmesartan, a novel AT1 antagonist, suppresses cytotoxic myocardial injury in autoimmune heart failure. *Am J Physiol Heart Circ Physiol* 2005; **289**: H1147–H1152.
15. Miyata T, van Ypersele de Strihou C, Ueda Y, *et al*: Angio-

tensin II receptor antagonists and angiotensin-converting enzyme inhibitors lower *in vitro* the formation of advanced glycation end products: biochemical mechanisms. *J Am Soc Nephrol* 2002; **13**: 2478–2487.
16. Anraku M, Kitamura K, Shinohara A, *et al*: Intravenous iron administration induces oxidation of serum albumin in hemodialysis patients. *Kidney Int* 2004; **66**: 841–848.
17. Shimada H, Kitamura K, Anraku M, *et al*: Effect of telmisartan on ambulatory blood pressure monitoring, plasma brain natriuretic peptide, and oxidative status of serum albumin in hemodialysis patients. *Hypertens Res* 2005; **28**: 987–994.
18. Mera K, Anraku M, Kitamura K, *et al*: Oxidation and carboxy methyl lysine-modification of albumin: possible involvement in the progression of oxidative stress in hemodialysis patients. *Hypertens Res* 2005; **28**: 973–980.
19. Gay CA, Gebicki JM: Measurement of protein and lipid hydroperoxides in biological systems by the ferric-xylenol orange method. *Anal Biochem* 2003; **315**: 29–35.
20. Shacter E, Williams JA, Lim M, Levine RL: Differential susceptibility of plasma proteins to oxidative modification: examination by western blot immunoassay. *Free Radic Biol Med* 1994; **17**: 429–437.
21. Descamps-Latscha B, Witko-Sarsat V: Importance of oxidatively modified proteins in chronic renal failure. *Kidney Int* 2001; **59** (Suppl 78): S108–S113.
22. Daschner M, Lenhartz H, Botticher D, *et al*: Influence of dialysis on plasma lipid peroxidation products and antioxidant levels. *Kidney Int* 1996; **50**: 1268–1272.
23. Witko-Sarsat V, Gausson V, Nguyen AT, *et al*: AOPP-induced activation of human neutrophil and monocyte oxidative metabolism: a potential target for *N*-acetylcysteine treatment in dialysis patients. *Kidney Int* 2003; **64**: 82–91.
24. Witko-Sarsat V, Gausson V, Descamps-Latscha B: Are advanced oxidation protein products potential uremic toxins? *Kidney Int* 2003; **63** (Suppl 84): S11–S14.
25. Witko-Sarsat V, Friedlander M, Capeillere-Blandin C, *et al*: Advanced oxidation protein products as a novel marker of oxidative stress in uremia. *Kidney Int* 1996; **49**: 1304–1313.
26. Odetti P, Garibaldi S, Gurreri G, Aragno I, Dapino D: Protein oxidation in hemodialysis and kidney transplantation. *Metabolism* 1996; **45**: 1319–1322.
27. Himmelfarb J, McMonagle E: Albumin is the major plasma protein target of oxidant stress in uremia. *Kidney Int* 2001; **60**: 358–363.
28. Bourdon E, Loreau N, Blache D: Glucose and free radicals impair the antioxidant properties of serum albumin. *FASEB J* 1999; **13**: 233–244.
29. Gebicki JM: Protein hydroperoxides as new reactive oxygen species. *Redox Rep* 1997; **3**: 99–110.
30. Mera K, Anraku M, Kitamura K, Nakajou K, Maruyama T, Otagiri M: The structure and function of oxidized albumin in hemodialysis patients: its role in elevated oxidative stress *via* neutrophil burst. *Biochem Biophys Res Commun* 2005; **334**: 1322–1338.
31. Sogami M, Nagaoka S, Era S, Honda M, Noguchi K: Resolution of human mercapt- and nonmercaptalbumin by high-performance liquid chromatography. *Int J Pept Protein Res* 1984; **24**: 96–103.
32. Hayakawa A, Kuwata K, Era S, *et al*: Alteration of redox state of human serum albumin in patients under anesthesia and invasive surgery. *J Chromatogr B Biomed Sci Appl* 1997; **698**: 27–33.
33. Sogami M, Era S, Nagaoka S, *et al*: High-performance liquid chromatographic studies on non-mercapt in equilibrium with mercapt conversion of human serum albumin. *J Chromatogr* 1985; **332**: 19–27.
34. Suzuki E, Yasuda K, Takeda N, *et al*: Increased oxidized form of human serum albumin in patients with diabetes mellitus. *Diabetes Res Clin Pract* 1992; **18**: 153–158.
35. Soejima A, Kaneda F, Manno S, *et al*: Useful markers for detecting decreased serum antioxidant activity in hemodialysis patients. *Am J Kidney Dis* 2002; **39**: 1040–1046.
36. Soriani M, Pietraforte D, Minetti M: Antioxidant potential of anaerobic human plasma: role of serum albumin and thiols as scavengers of carbon radicals. *Arch Biochem Biophys* 1994; **312**: 180–188.
37. Stamler JS, Simon DI, Osborne JA, *et al*: *S*-Nitrosylation of proteins with nitric oxide: synthesis and characterization of biologically active compounds. *Proc Natl Acad Sci U S A* 1992; **89**: 444–448.
38. Unger T, Culman J, Gohlke P: Angiotensin II receptor blockade and end-organ protection: pharmacological rationale and evidence. *J Hypertens Suppl* 1998; **16**: S3–S9.
39. Rajagopalan S, Duquaine D, King S, Pitt B, Patel P: Mineralocorticoid receptor antagonism in experimental atherosclerosis. *Circulation* 2002; **105**: 2212–2216.
40. Yao L, Kobori H, Rahman M, *et al*: Olmesartan improves endothelin-induced hypertension and oxidative stress in rats. *Hypertens Res* 2004; **27**: 493–500.

0090-9556/08/3601-81–86$20.00
DRUG METABOLISM AND DISPOSITION

DMD 36:81–86, 2008

Vol. 36, No. 1
16873/3285340
Printed in U.S.A.

# Subdomain IIIA of Dog Albumin Contains a Binding Site Similar to Site II of Human Albumin

Ken-ichi Kaneko, Hikaru Fukuda, Victor Tuan Giam Chuang, Keishi Yamasaki, Kohichi Kawahara, Hitoshi Nakayama, Ayaka Suenaga, Toru Maruyama, and Masaki Otagiri

*Graduate School of Pharmaceutical Sciences, Kumamoto University, Kumamoto, Japan (K.K., H.F., K.K., H.N., A.S., T.M., M.O.); School of Pharmacy, Curtin University of Technology, Perth, Western Australia, Australia (V.T.G.C.); and Graduate School of Pharmaceutical Sciences, Sojo University, Kumamoto, Japan (K.Y.)*

Received May 25, 2007; accepted October 4, 2007

**ABSTRACT:**

**Dog albumin contains a specific drug-binding site that binds most of the site II ligands of human albumin. This study was undertaken to elucidate the structural configuration of this binding site using a photoaffinity labeling technique. Dog albumin and albumins of other animal species were photolabeled with [$^{14}$C]ketoprofen. The photolabeled albumins were cleaved with cyanogen bromide (CNBr) and analyzed autoradiographically after electrophoretic separation. A 11.6-kDa CNBr fragment of the photolabeled dog albumin was found to have incorporated most of the radioactivity. Site II ligands of human albumin inhibited photoincorporation of radioactivity to this fragment. The binding constants of human and dog albumins ranged from 10 to 12 × $10^5$ $M^{-1}$, at least twice as high as those of rat, rabbit, and bovine albumins. Edman degradation was performed to elucidate the amino acid sequence of the photolabeled peptide derived from further digestion of the dog 11.6-kDa CNBr fragment with lysyl endopeptidase. The sequence was XXSESLVXRX, which corresponds to Cys$^{476}$-Arg$^{485}$ of dog albumin. Dog albumin contains a binding site that may have a binding microenvironment similar to that of site II on human albumin. Therefore, dog may be a better experimental animal for data extrapolation from animal to human with regard to site II drug-drug interactions.**

The binding of drugs in human plasma, in most cases, is caused mainly by binding to albumin because albumin is normally present at high concentrations of approximately 40 mg/ml (0.6 mM) in healthy human subjects (Peters, 1996; Davi et al., 1999) and also by the presence of high-affinity binding sites in the protein. In some cases, albumin binding will influence the pharmacodynamic activity of the drug also (Lewis et al., 2006). Determination of the distribution and plasma protein binding of a drug for species used in preclinical safety investigations and characterization of the interaction of the drug with human albumin can be critical for its pharmacokinetics and are needed for a comparison of pharmacokinetics across species (Kosa et al., 1997; Weiss et al., 2006). Research on species differences in albumin binding of drugs has been done, but in most cases only the binding characteristics were investigated, with very few studies on the binding sites of albumins of different species (Mizojiri et al., 1997; Nonaka et al., 2003; Acharya et al., 2006). Hence, elucidation of the drug-binding sites on albumins of different species will provide useful information when drug interactions with animal models are investigated.

Albumins bind endogenous as well as exogenous substances including drugs (Peters, 1996; Petersen et al., 2002; Simard et al., 2006). There are at least two discrete drug-binding sites on human albumin, namely, site I and site II, according to the classification of Sudlow et al. (1975). Crystallographic analysis of human albumin confirms the locations of the two binding sites I and II at domains II and III, respectively (Petitpas et al., 2003; Ghuman et al., 2005). We have previously reported that rat, rabbit, and bovine albumins contain a binding site similar to site I of human albumin, whereas dog albumin contains a binding site similar to site II of human albumin using ibuprofen and diazepam as the site II probes (Kosa et al., 1997). However, the conclusion was made on the basis of the results of a fluorescent probe displacement experiment, which did not address the location of binding sites on the protein molecule. In addition, at present only crystallographic structures of human and horse albumins are available (Ho et al., 1993; Curry et al., 1998). The lack of structural data for albumins of other animal species has, to a certain extent, impeded further assessment of drug-binding models.

In a previous study, we had successfully identified the binding site of ketoprofen (KP) on human albumin. KP is a site II ligand of human albumin that can be used as a labeling agent because of its benzophenone moiety. In that study, the binding site structural configuration of site II of human albumin was found to consist of Cys$^{476}$-Pro$^{499}$ which forms part of subdomain IIIA of human albumin (Chuang et al., 1999). Hence, to identify the location of the KP binding site on dog albumin, [$^{14}$C]KP was used to photolabel dog albumin and the amino acid sequence of the photolabeled dog albumin peptide was determined.

Article, publication date, and citation information can be found at http://dmd.aspetjournals.org.
doi:10.1124/dmd.107.016873.

**ABBREVIATIONS:** KP, ketoprofen; PAGE, polyacrylamide gel electrophoresis; CNBr, cyanogen bromide; TFA, trifluoroacetic acid; WF, warfarin; OCT, sodium octanoate; DZP, diazepam; IP, ibuprofen; HPLC, high-performance liquid chromatography; Lys-C, lysyl endopeptidase; PVDF, polyvinylidene diflouride; CD, circular dichroism; HSA, human serum albumin; UCN-01, 7-hydroxystaurosporine.

## Materials and Methods

**Materials.** Human, dog, rat, rabbit, and bovine albumins were obtained from Sigma-Aldrich (St. Louis, MO). Before all experiments, all albumins were defatted with activated charcoal in solution at 4°C, acidified with HCl to pH 3 and then lyophilized. The albumins used in this study showed only one band of approximately 66 kDa in SDS-PAGE. [$^{14}$C]KP (12.95 $\mu$Ci/mmol) was obtained from Hisamitsu Pharmaceutical Co., Inc., Tosu Laboratories (Saga, Japan). Cyanogen bromide (CNBr), dithiothreitol, and trifluoroacetic acid (TFA) were obtained from Nacalai Tesque (Kyoto, Japan). Warfarin (WF) was obtained from Eisai Co., Ltd. (Tokyo, Japan). Sodium octanoate (OCT) was obtained from Wako Pure Chemical Industries, Ltd. (Osaka, Japan). Diazepam (DZP) was obtained from Sumitomo Pharmaceuticals Co., Ltd. (Osaka, Japan). Ibuprofen (IP) was obtained from Kaken Pharmaceutical Co., Ltd. (Tokyo, Japan). All other chemicals were of analytical grade.

**Photoaffinity Labeling of Albumins with [$^{14}$C]KP.** Albumin (50 $\mu$M) was incubated with [$^{14}$C]KP (25 $\mu$M) in the absence and presence of WF, IP, OCT, and DZP (250 $\mu$M), in 100 $\mu$l of 20 mM Tris buffer, at pH 7.4 in a 1.5-ml Eppendorf tube at room temperature in the dark for 60 min. The incubation mixture was then placed on ice and irradiated for 30 min at a wavelength of longer than 320 nm by a 100-W black light/blue lamp (Ultra-Violet Products, Inc., San Gabriel, CA) at a distance of 10 cm. After irradiation, the photolabeled albumins were precipitated by adding 1 ml of acetone, followed by centrifugation at 15,000 rpm for 10 min. The pellet was reductively pyridylethylated.

**Reductive Pyridylethylation.** One hundred microliters of the reduction medium (6 M guanidinium HCl, 1 M Tris buffer, pH 8.0, 20 mM EDTA, and 100 mM dithiothreitol) was added to the pellet, which was then incubated under $N_2$ at 37°C for at least 12 h. After the addition of 1 $\mu$l of 4-vinylpyridine, the mixture was incubated under $N_2$ for an additional 30 min at room temperature in the dark. At the end of the pyridylethylation reaction, 1 ml of acetone and 100 $\mu$l of 0.1% TFA was added to the mixture to terminate the reaction. The suspension was then vortexed vigorously followed by a light centrifugation. One milliliter of ethanol was added, the mixture was further vortexed to remove the salts and unreacted 4-vinylpyridine, and the suspension was centrifuged at 15,000 rpm for 10 min.

**CNBr Cleavage and Tricine SDS-PAGE.** The pyridylethylated pellet was dissolved in 100 $\mu$l of CNBr in 70% formic acid (CNBr-methionine residues = 200:1) and incubated under $N_2$ for 24 h in the dark at room temperature. 1 ml of Milli-Q water was added at the end of the CNBr cleavage to stop the reaction, and the resulting mixture was lyophilized. The lyophilized CNBr fragments were resuspended in 100 $\mu$l of 0.1% TFA, and the protein concentration was determined by a Bradford assay in which 6.5 $\mu$g of the fragment mixture was applied to each lane of the gel with separation using Tricine SDS-PAGE.

**Autoradiographic Analysis.** For autoradiographic analysis, the dried SDS-PAGE gel was placed in contact with an imaging plate (BAS III; Fuji Film Co., Tokyo, Japan) in a cassette (BAS cassette 2040; Fuji Film Co.) at room temperature for 48 h. The imaging plate was scanned and analyzed using a Bio-Imaging Analyzer (model BAS FLA-3000 G; Fuji Film Co.) and was then analyzed using L Process V 1.6 software (Fuji Film Science Lab 98; Fuji Film Co.). The incorporation of radioactivity into individual fragments was quantified using Image Gauge V 3.1 software (Fuji Film Co.).

**Capillary HPLC Separation and Sequence Analysis.** The 11.6-kDa CNBr peptide of dog albumin was eluted from the gel after Tricine SDS-PAGE with an Electro-Eluter (model 422; Bio-Rad, Hercules, CA). The peptide was then digested with the enzyme lysyl endopeptidase (Lys-C) in 20 mM ammonium bicarbonate at 37°C for 16 h. Ten microliters of the digestion sample was then injected onto the ABI 173 A MicroBlotter Capillary HPLC System (PerkinElmer Life and Analytical Sciences, Waltham, MA). The sample was manipulated following the manufacturer's instructions. The blotted membrane from the capillary HPLC separation was in contact with an imaging plate for 48 h before autoradiographic analysis. The PVDF membrane was positioned with the chromatogram of a peptide map from the ABI 173 A MicroBlotter Capillary HPLC System. A portion of the PVDF membrane was excised for sequencing with reference to the autoradiogram. Edman degradation of the photolabeled peptide was carried out with a Procise Sequencer (Applied Biosystems, Foster City, CA).

TABLE 1

*Binding parameters of KP to different serum albumins at pH 7.4*

Results were determined by ultrafiltration. Values represent the mean ± S.D.

| | $n_1$ | $K_1$ ($\times 10^5$ $M^{-1}$) | $n_2$ | $K_2$ ($\times 10^4$ $M^{-1}$) |
|---|---|---|---|---|
| Human | 1.34 ± 0.04 | 10.02 ± 0.47 | 4.82 ± 0.16 | 2.11 ± 0.13 |
| Dog | 0.91 ± 0.01 | 11.65 ± 0.21 | 7.09 ± 0.62 | 0.66 ± 0.09 |
| Bovine | 1.72 ± 0.13 | 4.62 ± 0.48 | 5.46 ± 0.59 | 1.16 ± 0.30 |
| | | $n$ | $K$ ($\times 10^5$ $M^{-1}$) | |
| Rat | | 3.32 ± 0.05 | 2.45 ± 0.06 | |
| Rabbit | | 2.93 ± 0.05 | 3.20 ± 0.15 | |

**Determination of Binding Parameters.** To quantitatively analyze the binding mode, binding parameters were determined by ultrafiltration. Ultrafiltration was performed using Ultrafree MC (Amicon Division, Danvers, MA). Ligands were added to 400 $\mu$l of albumins (10 $\mu$M) in 20 mM Tris buffer, at pH 7.4, and preincubated at 25°C for 30 min before centrifugation (2000 rpm for 20 min). To determine the free ligand concentrations ($C_f$), a 200-$\mu$l aliquot of the filtrate was added to 2 ml of scintillation cocktail in a scintillation vial (Pyrex; Asahi Techno Glass Corporation, Chiba, Japan), vortexed, and counted by using a scintillation counter (LSC-5121, Aloka Co., Ltd, Tokyo, Japan). No adsorption of the ligands to membrane or apparatus was detectable.

Binding parameters were determined by fitting the experimental data to the following equation using a nonlinear least-squares program (MULTI program):

$$r = \sum_{i=1}^{m} \frac{n_i K_i C_f}{1 + K_i C_f} \qquad (1)$$

where $n_i$ is the number of binding sites, $K_i$ is the binding constant in the $i$th binding class, and $r$ is the moles of bound ligand per mole of total protein ($C_b/P_t$).

**CD Spectra Measurements in the Presense of KP.** CD spectra were measured using a JASCO J-820 spectropolarimeter (JASCO, Tokyo, Japan) at 25°C with a 10-mm path length cell. The concentration of various albumins was 60 $\mu$M and the KP concentration was 100 $\mu$M in 20 mM Tris-HCl buffer (pH 7.4). The scan speed was adjusted at 10 nm/min and was the average of three scans, with the range of wavelength scanned from 300 to 400 nm. The results were represented as observed ellipticity ($\theta_{obs}$) in millidegrees. Induced CD was determined as the CD of the albumin-KP mixture after subtraction of CD of the albumin alone.

## Results

**Binding Parameters of KP to Albumins of Different Species.** The number of binding sites and the corresponding binding constants for binding of KP to albumins were estimated using ultrafiltration (Table 1; Fig. 1). The primary binding constants of human and dog albumins ranged from 10 to 12 $\times$ $10^5$ $M^{-1}$, at least twice as high as those of rat, rabbit, and bovine albumins, which ranged within 2 to 5 $\times$ $10^5$ $M^{-1}$. In human, dog, and bovine albumins, KP binds at primary and secondary sites. On the other hand, in rat and rabbit albumins, KP binds to three sites that could not be categorized into primary or secondary level.

**CD Spectra Measurements of Albumins in the Presence of KP.** When KP binds to HSA, a specific Cotton effect will be induced (Dubois et al., 1994; Zandomeneghi, 1995). Figure 2 shows the CD spectra obtained when KP was added to the different albumin solutions. Binding of KP to human and dog albumins resulted in a negative Cotton effect, with a maximum at approximately 340 nm. Binding of KP to rabbit albumin led to a decrease in the specific negative Cotton effect compared with those induced in human and dog albumins. Meanwhile, the spectrum of bovine albumin-KP binding was appreciably different from those of human, dog, and rabbit

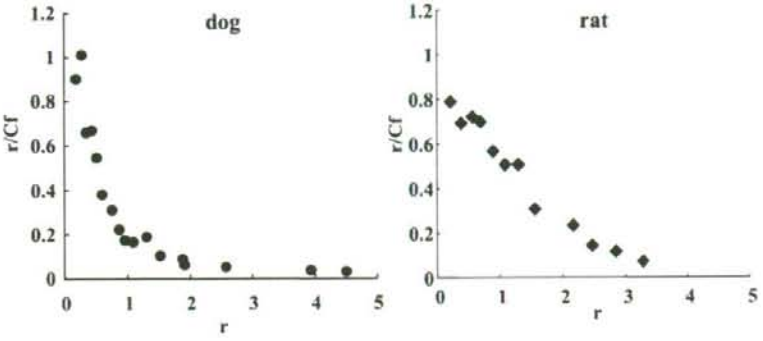


FIG. 1. Scatchard plots of the binding of KP to dog (●) and rat (◆) albumins.

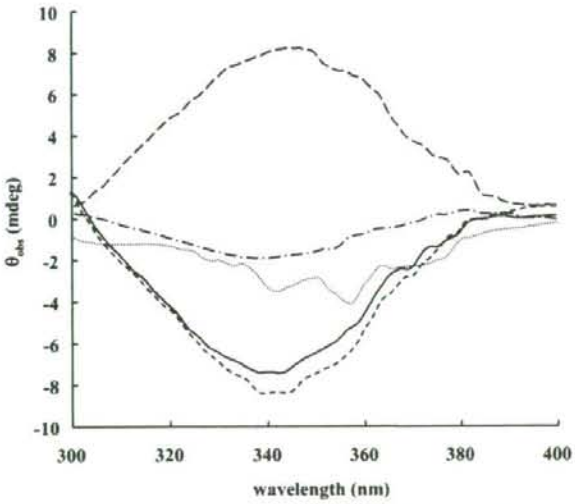


FIG. 2. CD spectra of different albumins in the presence of KP at 25°C. The sample solutions contained 100 μM KP and 60 μM albumin in 20 mM Tris-HCl buffer (pH 7.4). ——, human albumin; ····, dog albumin; - - -, rat albumin; –·–, rabbit albumin; – – –, bovine albumin.

albumins. With an effect different from that of other albumins, binding of KP to rat albumin resulted in a positive Cotton effect.

**Photolabeling of Albumins of Various Species with [$^{14}$C]KP.** The autoradiogram in Fig. 3 shows that the radioactivity band appeared only upon photoirradiation of albumins with [$^{14}$C]KP. Absence of a radioactive band in the samples without irradiation indicated that no covalent attachment of KP to albumin occurred in the dark. Human and dog albumins appeared to incorporate radioactivity to a greater extent than the other albumins.

**CNBr Fragments of Albumins of Various Species Photolabeled with [$^{14}$C]KP.** Human and rat albumins have six, whereas dog and bovine albumins contain four methionine residues. Rabbit albumin contains only one methionine residue (Fig. 4). Because the amino acid sequence of each albumin is available, CNBr cleavage products of these albumin can be identified by their mobilities on SDS-containing gels in relation to their molecular weights. Thus, it is possible to preview which subdomain is photolabeled via inspection of the radioactivity intensity of each band (Fig. 5). Significant radioactivity could be observed for the 11.6-kDa CNBr fragments of the photolabeled human and dog albumins and 15.3-kDa bovine albumin was found to have incorporated most of the radioactivity. On the other hand, only a comparatively low level of radioactivity could be ob-

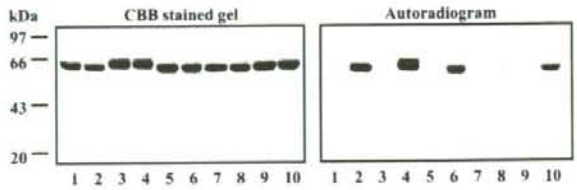


FIG. 3. Photolabeling of different albumins (1, 2, human; 3, 4, dog; 5, 6, rat; 7, 8, rabbit; 9, 10, bovine) with [$^{14}$C]KP. Lanes 1, 3, 5, 7, and 9, sample taken just before photoirradiation. Lanes 2, 4, 6, 8, and 10, sample taken after 30 min of irradiation

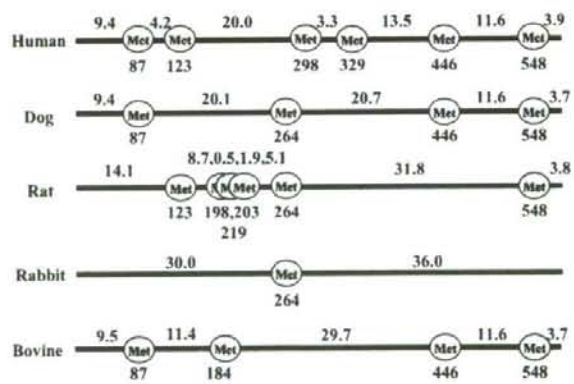


FIG. 4. The position of methionine residues on different albumins. The numbers above the line are calculated molecular weights. The numbers below "Met" are the positions of methionine residues in the amino acid sequence.

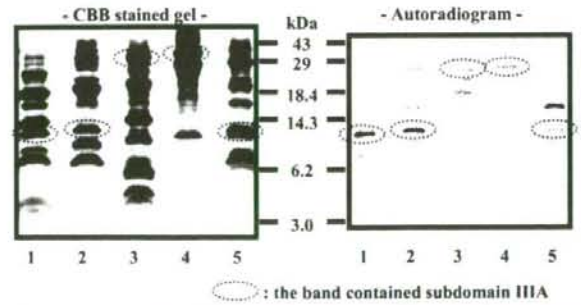


FIG. 5. CNBr fragments of different albumins after [$^{14}$C]KP photoaffinity labeling separated by Tricine gel electrophoresis and the corresponding autoradiogram. 1, human (11.6 kDa); 2, dog (11.6 kDa); 3, rat (31.8 kDa), 4, rabbit (36.0 kDa), 5, bovine (11.6 kDa).

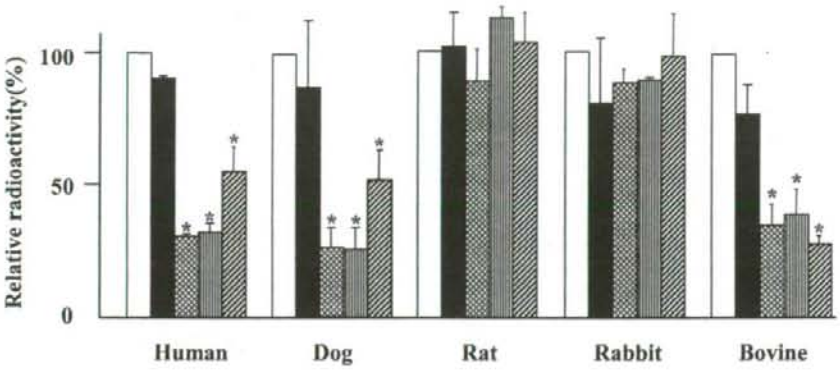


FIG. 6. Autoradiogram and relative radioactivity of the bands containing subdomain IIIA after photoirradiation in the presence of various competitors. The photolabeled albumins were cleaved with CNBr and separated with Tricine gel electrophoresis. The final concentration ratio for different albumins, [$^{14}$C]KP and competitors was 1:0.5:5. □, control; ■, WF; ▩, OCT; ▨, DZP; and ▧, IP. Data are expressed as means ± S.D. ($n$ = 3–4). *, $p < 0.01$, compared with control.

served for the 31.8-kDa CNBr fragments of the photolabeled rat albumin and 36.0-kDa peptide of rabbit albumin.

**Photolabeling Inhibition by Site I and II Ligands of Human Albumin.** To determine the presence of a binding site, the specificity of the photolabeling of [$^{14}$C]KP to albumins was further investigated by competition experiments. The peptide-containing subdomain IIIA has a molecular mass of 11.6 kDa for human, dog, and bovine albumins, 31.8 kDa for rat albumin, and 36.0 kDa for rabbit albumin. In the absence of a competitor, the extent of radioactivity incorporation of the peptide containing subdomain IIIA for each albumin was the same as the result in Fig. 5. KP binds primarily to site II of human albumin. Site II ligands, IP, DZP, and OCT, as well as a site I ligand, WF, were used as competitors in photolabeling albumins with [$^{14}$C]KP. The extent of photolabeling inhibition was expressed as a percentage of the control. A decrease in the radioactivity of the peptide containing subdomain IIIA reflects the inhibition of photoincorporation of [$^{14}$C]KP by the competitor. In the presence of DZP and OCT, the intensity of the 11.6-kDa band of human and dog albumins decreased to an extent greater than that in the presence of IP. On the other hand, IP, DZP, and OCT reduced the radioactivity intensity of the 11.6-kDa band of bovine albumin to the same extent. WF did not appear to affect the intensity of the band containing subdomain IIIA (Fig. 6).

**Determination of the Photolabeled Peptide Amino Acid Sequence of Dog Albumin.** The 11.6-kDa CNBr peptide from dog albumin was subjected to further digestion with Lys-C to locate more precisely which region of subdomain IIIA was photolabeled by KP. The peptides generated from the second digestion were separated and simultaneously blotted onto a strip of PVDF membrane with a capillary HPLC system. One radioactivity spot corresponding to one peak was obtained (Fig. 7, A and B). The amino acid sequence of the photolabeled fragment after further digestion with Lys-C was XX-SESLVXRX, which corresponds to the sequence Cys$^{476}$-Arg$^{485}$ of dog albumin (Fig. 7C).

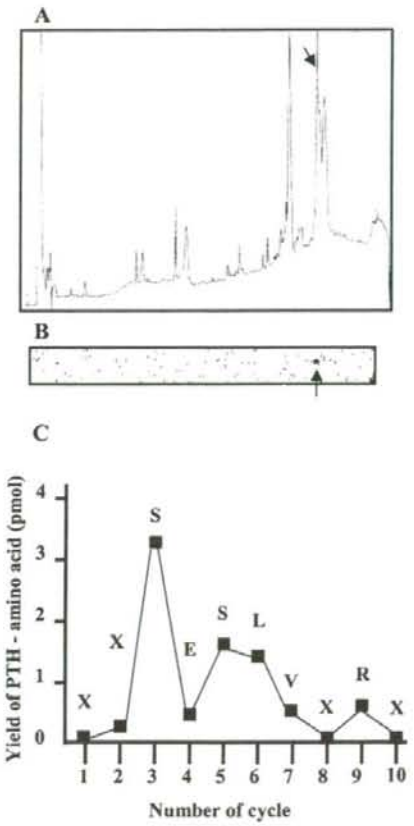


FIG. 7. Chromatogram of capillary HPLC (A), autoradiogram of blotted PVDF membrane of dog albumin digested with endopeptidase Lys-C (B), and N-terminal amino acid sequence analysis by Edman degradation method and amino acid sequence of the photolabeled region of dog albumin (C). Arrows in (A) and (B) indicate photolabeled peptide peak and radioactivity spot, respectively. PTH, phenylthiohydantoin.

## Discussion

High binding affinity to a plasma protein may cause a drug to be retained in the plasma and to not be readily distributed to the tissue for therapeutic action to take place. The high degree of binding of UCN-01 to human $\alpha_1$-acid glycoprotein, which causes a reduction in its distribution and clearance, resulting in high plasma concentrations in humans has been reported (Fuse et al., 1998). Moreover, we reported previously that species differences observed with phenylbutazone have an impact on the in vivo serum protein binding of sulfadimethoxine (Imamura et al., 1986).

In the process of drug development, preclinical animal trials are required to examine the safety and efficacy of the candidate drug. From the animal experiments, drug protein binding and distribution data are important for comparison of the pharmacokinetics of drugs across species and for interspecies scaling. Such comparisons will allow meaningful referencing of pharmacokinetic parameters to either

blood or plasma concentrations of the drug. Therefore, further refinement of the animal experimental design via selection of appropriate experimental animal based upon the drug class and the expected interacting proteins is desirable.

Despite the fact that the primary structure of the serum albumins of various species are highly homologous (approximately 80% homology between human and the species used in this study), drug-binding properties differ considerably among species. We reported that dog albumin is suitable for investigating drug-drug interactions on site II, whereas rat, rabbit, and bovine albumins are suitable for examining the binding of site I drugs (Kosa et al., 1997). Based on that study we attempted to elucidate the structural configuration of the binding site of dog albumin that resembles site II of HSA, using a photoaffinity labeling method (Garabedian and Yount, 1991; Chuang et al., 1999; DeSantis et al., 2000; Katsuki et al., 2005).

The usefulness of KP as a photoaffinity labeling agent and as a probe for identifying drug-binding sites on human albumin has been established previously (Chuang et al., 1999). To our knowledge, this study is the first to report identification of the presence of binding sites in various experimental animal albumins using the photoaffinity labeling technique. The extent of photoincorporation of [$^{14}$C]KP to each albumin was in accordance with the binding experiment result obtained with ultrafiltration and CD spectra measurements in the presence of KP (Table 1; Fig. 3). Moreover, these results are in agreement with the binding experiments using IP that we reported previously (Kosa et al., 1997) (Table 1; Figs. 1–3). The primary binding constant of KP to human albumin was similar to that reported by Rahman et al. (1993).

Autoradiographic analysis of CNBr fragments of human albumin photolabeled with [$^{14}$C]KP indicated that a 11.6-kDa peptide corresponding to Pro$^{447}$-Met$^{548}$ contained the highest radioactivity. This sequence was found to form the binding pocket of site II in subdomain IIIA of human albumin. Dog and bovine albumins will also derive a peptide with a molecular mass of 11.6 kDa upon CNBr cleavage, as could be deduced from the amino acid sequences (Met$^{446}$-Met$^{548}$) of these two albumins. The CNBr peptides of rat and rabbit containing the sequence with high homology and that of the human albumin 11.6-kDa CNBr peptide were Met$^{264}$-Met$^{548}$ (31.8 kDa) and Met$^{264}$-Glu$^{584}$ (36 kDa), respectively (Fig. 4). As shown in Fig. 5, only the 11.6-kDa CNBr peptide of dog albumin incorporated radioactivity to an extent comparable to that of human albumin. Interestingly, the corresponding peptide of bovine albumin did not incorporate a significant extent of the radioactivity. Instead, a peptide with an estimated molecular mass of 15.3 kDa exhibited a higher level of radioactivity. Edman degradation of this peptide revealed an amino acid sequence starting from Pro$^{447}$ (data not shown), indicating that the peptide might derive from an incomplete cleavage of CNBr, which resulted in a peptide with a sequence starting from Pro$^{447}$-Ala$^{584}$. It is very likely that Met$^{548}$ of bovine albumin could have been photolabeled by [$^{14}$C]KP, resulting in its resistance to CNBr cleavage.

Such a discrepancy could be due to a difference in the amino acid sequence that would notably influence the secondary as well as the tertiary structures of the albumins. The induced CD spectra for KP binding (Fig. 2) and the intrinsic CD spectra for albumins themselves showed a difference between human albumin and bovine albumin (data not shown), in agreement with the results reported by Kosa et al. (1997). Hence, human, dog, and bovine albumins contain a binding site of KP in subdomain IIIA, but the binding site structural configuration of bovine albumin is somewhat different from those of human and dog albumins.

IP, DZP, and OCT, site II ligands of human albumin, were able to inhibit the binding of KP to the primary binding sites of dog and bovine albumins. However, the inhibition pattern suggested that KP interacted with dog albumin in a manner similar to that for human albumin but different from that for bovine albumin (Fig. 6). In a previous study, we reported that bovine albumin has no primary but only a secondary binding site for DZP (Kosa et al., 1997). Hence, this secondary binding site of DZP might overlap with the binding site of KP on bovine albumin. The inhibition pattern of human albumin and hence that of dog albumin by IP, DZP, and OCT could be explained from the crystal structures of the drug-HSA complex (Ghuman et al., 2005). We previously reported that the hydrophobic moiety of *R*-KP interacts with Arg$^{485}$ (Chuang et al., 1999). In the IP-human albumin complex crystal structures, IP binds in the site II binding pocket in such a way that its hydrophobic moiety was away from Arg$^{485}$ in contrast to DZP, which binds near to Arg$^{485}$ (Ghuman et al., 2005). Bhattacharya et al. (2000) proposed that two molecules of medium chain fatty acids, including OCT, bind to site II and one of the two molecules forms hydrogen bond to Arg$^{485}$. This proposal may provide an explanation for the observation that IP inhibited KP binding to a lesser extent than did DZP and OCT.

TABLE 2

*The amino acid sequence of peptide (476–499) of albumin of different species*

| Species | Peptide of 476–499 | Homology | Primary Binding Sites | |
|---|---|---|---|---|
| | | % | | |
| Human | CCTESLVNRRPCFSALEVDETYVPK | | IP* | DZP* |
| Dog | CCSESLVNRRPCFSGLEVDETYVPK | 91.7 | O | O |
| Bovine | CCTESLVNRRPCFSALTPDETYVPK | 91.7 | O | X |
| Rat | CCSGSLVERRPCFSALTVDETYVPK | 83.3 | O | X |
| Rabbit | CCSESLSNRRPCFSALGPDETYVPK | 83.3 | O | X |

* Kosa et al., 1997.

Amino acid sequence analysis of the photolabeled peptide of dog albumin after further digestion with Lys-C enzyme indicated a sequence corresponding to the sequence Cys$^{476}$-Pro$^{499}$ of dog albumin (Fig. 7C). In a previous study, we reported that Cys$^{476}$-Pro$^{499}$ in subdomain IIIA (site II) of human albumin was the region photolabeled by KP (Chuang et al., 1999). Sequence homology comparison of this Cys$^{476}$-Pro$^{499}$ peptide of human albumin (Chuang et al., 1999) and dog albumin (Fig. 7C), with all other albumins used in the study showed that dog and bovine albumin has the highest homology (91.7%) with human albumin. As shown in Table 2, human and dog albumins have Glu$^{492}$ and Val$^{493}$, but bovine albumin does not. Moreover, DZP, a site II ligand, binds to dog albumin with high affinity but only binds to bovine albumin with much lower affinity (Kosa et al., 1997). Thus, Glu$^{492}$ and Val$^{493}$ in human and dog albumins are important residues that constitute the structure of the site II binding site. In addition, the induced CD spectra of the human albumin-KP complex agreed with that of the dog albumin-KP complex (Fig. 2). The CD spectra of these albumins indicated that the secondary and tertiary structures of dog albumin were almost the same as those of human albumin (data not shown). Therefore, dog albumin contains a binding site located in subdomain IIIA exhibiting a structural configuration of binding similar to that of site II of human albumin.

In conclusion, in the preclinical animal experiments, dog may be a better candidate animal for examination of the protein binding as well as distribution of site II drugs.

**Acknowledgments.** We thank members of Kumamoto University Institute of Resource Development and Analysis Radioisotope Center.

## References


Acharya MR, Sparreboom A, Sausville EA, Conley BA, Doroshow JH, Venitz J, and Figg WD (2006) Interspecies differences in plasma protein binding of MS-275, a novel histone deacetylase inhibitor. *Cancer Chemother Pharmacol* **57**:275–281.

Bhattacharya AA, Grune T, and Curry S (2000) Crystallographic analysis reveals common modes of binding of medium and long-chain fatty acids to human serum albumin. *J Mol Biol* **303**:721–732.

Chuang VT, Kuniyasu A, Nakayama H, Matsushita Y, Hirono S, and Otagiri M (1999) Helix 6 of subdomain III A of human serum albumin is the region primarily photolabeled by ketoprofen, an arylpropionic acid NSAID containing a benzophenone moiety. *Biochim Biophys Acta* **1434**:18–30.

Curry S, Mandelkow H, Brick P, and Franks N (1998) Crystal structure of human serum albumin complexed with fatty acid reveals an asymmetric distribution of binding sites. *Nat Struct Biol* **5**:827–835.

Davi H, Tronquet C, Caix J, Simiand J, Briot C, Berger Y, and Thiercelin JF (1999) Disposition of tiludronate (Skelid) in animals. *Xenobiotica* **29**:1017–1031.

DeSantis G, Paech C, and Jones JB (2000) Benzophenone boronic acid photoaffinity labeling of subtilisin CMMs to probe altered specificity. *Bioorg Med Chem* **8**:563–570.

Dubois N, Lapicque F, Magdalou J, Abiteboul M, and Netter P (1994) Stereoselective binding of the glucuronide of ketoprofen enantiomers to human serum albumin. *Biochem Pharmacol* **48**:1693–1699.

Fuse E, Tanii H, Kurata N, Kobayashi H, Shimada Y, Tamura T, Sasaki Y, Tanigawara Y, Lush RD, Headlee D, et al. (1998) Unpredicted clinical pharmacology of UCN-01 caused by specific binding to human $\alpha_1$-acid glycoprotein. *Cancer Res* **58**:3248–3253.

Garabedian TE and Yount RG (1991) Direct photoaffinity labeling of gizzard myosin with vanadate-trapped adenosine diphosphate. *Biochemistry* **30**:10126–10132.

Ghuman J, Zunszain PA, Petitpas I, Bhattacharya AA, Otagiri M, and Curry S (2005) Structural basis of the drug-binding specificity of human serum albumin. *J Mol Biol* **353**:38–52.

Ho JX, Holowachuk EW, Norton EJ, Twigg PD, and Carter DC (1993) X-ray and primary structure of horse serum albumin (*Equus caballus*) at 0.27-nm resolution. *Eur J Biochem* **215**:205–212.

Imamura Y, Nakamura H, and Otagiri M (1986) Effect of phenylbutazone on serum protein binding of sulfadimethoxine in different animal species. *J Pharmacobiodyn* **9**:694–696.

Katsuki M, Chuang VT, Nishi K, Kawahara K, Nakayama H, Yamaotsu N, Hirono S, and Otagiri M (2005) Use of photoaffinity labeling and site-directed mutagenesis for identification of the key residue responsible for extraordinarily high affinity binding of UCN-01 in human $\alpha_1$-acid glycoprotein. *J Biol Chem* **280**:1384–1391.

Kosa T, Maruyama T, and Otagiri M (1997) Species differences of serum albumins: I. Drug binding sites. *Pharmacol Res* **14**:1607–1612.

Lewis RE, Wiederhold NP, Prince RA, and Kontoyiannis DP (2006) In vitro pharmacodynamics of rapid versus continuous infusion of amphotericin B deoxycholate against *Candida* species in the presence of human serum albumin. *J Antimicrob Chemother* **57**:288–293.

Mizojiri K, Okabe H, Sugeno K, Misaki A, Ito M, Kominami G, Esumi Y, Takaichi M, Harada T, Seki H, et al. (1997) Studies on the metabolism and disposition of the new retinoid 4-[(5,6,7,8-tetrahydro-5,5,8,8-tetramethyl-2-naphthyl)carbamoyl] benzoic acid. 4th communication: absorption, metabolism, excretion and plasma protein binding in various animals and man. *Arzneimittelforschung* **47**:259–269.

Nonaka K, Tsujioka T, Tougou K, and Mukai H (2003) Pharmacokinetics of the new pyrimidine derivative NS-7, a novel $Na^+/Ca^{2+}$ channel blocker. 1st communication: plasma concentrations and excretions after a single intravenous $^{14}C$-NS-7 injection to rats, dogs and monkeys. *Arzneimittelforschung* **53**:612–620.

Peters, T (1996) *All About Albumin*. Academic Press, San Diego.

Petersen CE, Ha CE, Curry S, and Bhagavan NV (2002) Probing the structure of the warfarin-binding site on human serum albumin using site-directed mutagenesis. *Proteins* **47**:116–125.

Petitpas I, Petersen CE, Ha CE, Bhattacharya AA, Zunszain PA, Ghuman J, Bhagavan NV, and Curry S (2003) Structural basis of albumin-thyroxine interactions and familial dysalbuminemic hyperthyroxinemia. *Proc Natl Acad Sci U S A* **100**:6440–6445.

Rahman MH, Yamasaki K, Shin YH, Lin CC, and Otagiri M (1993) Characterization of high affinity binding sites of non-steroidal anti-inflammatory drugs with respect to site-specific probes on human serum albumin. *Biol Pharm Bull* **16**:1169–1174.

Simard JR, Zunszain PA, Hamilton JA, and Curry S (2006) Location of high and low affinity fatty acid binding sites on human serum albumin revealed by NMR drug-competition analysis. *J Mol Biol* **361**:336–351.

Sudlow G, Birkett DJ, and Wade DN (1975) The characterization of two specific drug binding sites on human serum albumin. *Mol Pharmacol* **11**:824–832.

Weiss HM, Fresneau M, Camenisch GP, Kretz O, and Gross G (2006) In vitro blood distribution and plasma protein binding of the iron chelator deferasirox (ICL670) and its iron complex Fe-[ICL670]2 for rat, marmoset, rabbit, mouse, dog, and human. *Drug Metab Dispos* **34**:971–975.

Zandomeneghi M (1995) Circular dichroism of ketoprofen complexed to serum albumins: conformational selection by the protein: a novel optical purity determination technique. *Chirality* **7**:446–451.


**Address correspondence to:** Dr. Masaki Otagiri, Department of Biopharmaceutics, Graduate School of Pharmaceutical Sciences, Kumamoto University, 5-1 Oe-honmachi, Kumamoto 862-0973, Japan. E-mail: otagirim@gpo.kumamoto-u.ac.jp

Available online at www.sciencedirect.com
ScienceDirect
Biochemical and Biophysical Research Communications 364 (2007) 790–795
BBRC
www.elsevier.com/locate/ybbrc

# Effects of endogenous ligands on the biological role of human serum albumin in S-nitrosylation ☆

Yu Ishima [a], Takaaki Akaike [b], Ulrich Kragh-Hansen [c], Shuichi Hiroyama [a], Tomohiro Sawa [b], Toru Maruyama [a], Toshiya Kai [a], Masaki Otagiri [a,*]

[a] *Department of Biopharmaceutics, Graduate School of Pharmaceutical Sciences, Kumamoto University, 5-1 Oe-honmachi, Kumamoto 862-0973, Japan*
[b] *Department of Microbiology, Graduate School of Medical Sciences, Kumamoto University, 1-1-1 Honjo, Kumamoto 860-0811, Japan*
[c] *Department of Medical Biochemistry, University of Aarhus, DK-8000 Aarhus C, Denmark*

Received 9 October 2007
Available online 26 October 2007

**Abstract**

Many proteins have been identified as targets for S-nitrosylation, including structural and signaling proteins, and ion channels. S-nitrosylation plays an important role in regulating their activity and function. We used human serum albumin (HSA), a major endogenous NO traffic protein, and studied the effect of mediators on S-nitrosylation processes which control NO bioactivity. By using NOC-7, S-nitrosoglutathione, and activated RAW264.7 cells as NO-donors we found that high-affinity binding of endogenous ligands ($Cu^{2+}$, bilirubin and fatty acid) can affect these processes. It is likely that the same effects take place in many clinical situations characterized by increased fatty acid concentrations in plasma such as type II diabetes and the metabolic syndrome. Thus, endogenous ligands, changing their plasma concentrations, could be a novel type of mediator of S-nitrosylation not only in the case of HSA but also for other target proteins.


*Keywords:* Human serum albumin; Nitric oxide; Type II diabetes; Metabolic syndrome; Cysteine; S-Nitrosylation; Ligand binding; Fatty acids; Copper; Bilirubin

Post-translational modifications are essential in their functional regulation. Among these, changes of the redox state of cysteine residues are of great importance. The sulfhydryl moiety can interact with nitric oxide (NO) and thereby form S-nitrosothiols (RS-NO) [1–3]. RS-NOs may function as NO reservoirs and preserve the antioxidant and other activities of NO [4,5]. For example, it has been reported that S-nitroso human serum albumin (SNO-HSA) may serve in vivo as a circulating reservoir for NO produced by the endothelial cells [6]. The reservoir function was also reported to be operative when application of SNO-HSA to animals suffering from ischemia-reperfusion injury minimized the extent of tissue damage associated with reperfusion [7,8]. However, several pieces of evidence propose that RS-NOs are more than simply NO reservoirs [4]. Thus, the antibacterial and cytoprotective properties of SNO-HSAs [9] are most probably the results of S-transnitrosylation.

HSA is a single, non-glycosylated polypeptide that organizes to form a heart-shaped protein with approximately 67% α-helix but no β-sheet [10]. All but one (Cys-34) of the 35 cysteine residues are involved in the formation of

*Abbreviations:* HSA, human serum albumin; SNO-HSA, S-nitroso HSA; RS-NOs, S-nitrosothiols; GSH, glutathione; GS-NO, S-nitrosoglutathione; NOC-7, 1-hydroxy-2-oxo-3-(*N*-3-methyl-aminopropyl)-3-methyl-3′-triazene; OA, oleic acid; BR, bilirubin; DTT, 1,4-dithiothreitol; DTNB, 5,5′-dithiobis-2-nitrobenzoic acid; DTPA, diethylenetriaminepentaacetic acid; EDTA, ethylenediaminetetraacetic acid; PBS, phosphate-buffered saline; NEM, *N*-ethylmaleimide.

☆ This work was supported in part by Grants-in-Aid from the Japan Society for the Promotion of Science (JSPS), a Grant-in-Aid from the Ministry of Education, Culture, Sports, Science and Technology (18390051), Japan, and by Fonden af 1870.

* Corresponding author. Fax: +81 96 362 7690.
*E-mail address:* otagirim@gpo.kumamoto-u.ac.jp (M. Otagiri).

0006-291X/$ - see front matter © 2007 Elsevier Inc. All rights reserved.
doi:10.1016/j.bbrc.2007.10.094

stabilizing disulfide bonds. In the circulation, normally about half of the Cys-34 residues are freely accessible, i.e., not oxidized or involved in ligand binding, and they represent the largest fraction of free thiols in blood.

HSA is the most abundant protein in blood plasma and serves, among other things, as a transport and depot protein for numerous endogenous and exogenous compounds [10]. We studied the effects of the strongly bound ligands oleate (OA), bilirubin (BR) and $Cu^{2+}$ and the weakly bound ligands L-tryptophan, progesterone, ascorbate, $Zn^{2+}$ and $Fe^{2+}$ on S-nitrosylation of HSA by S-nitrosoglutathione (GS-NO), 1-hydroxy-2-oxo-3-(N-3-methyl-aminopropyl)-3-methyl-3′-triazene (NOC-7) and stimulated RAW264.7 cells.

## Materials and methods

*Materials.* Non-defatted HSA (96% pure) was donated by the Chemo-Sera-Therapeutic Research Institute (Kumamoto, Japan), and it was defatted by treatment with charcoal as described by Chen [11]. Sephadex G-25 (φ1.6 × 2.5 cm), Blue Sepharose CL-6B (φ2.5 × 20 cm), and RESOURCE PHE columns (φ0.64 × 3 cm) were from Amersham Pharmacia Biotech (Tokyo, Japan). Enzymes for DNA assays were from Takara (Kyoto, Japan). The Pichia Expression kit was from Invitrogen (Carlsbad, CA). L-Tryptophan, ascorbic acid, $FeCl_2$, $(CH_3COO)_2Zn$, $CuSO_4{\cdot}5H_2O$, BR, progesterone, OA, 1,4-dithiothreitol (DTT), and glutathione (GSH) were purchased from Sigma–Aldrich (St. Louis, MO). Sulfanilamide, naphthylethylenediamine–hydrochloride, $HgCl_2$ and $NaNO_2$ were obtained from Nakalai Tesque (Kyoto, Japan). GS-NO, NOC-7, 5,5′-dithiobis-2-nitrobenzoic acid (DTNB), diethylenetriaminepentaacetic acid (DTPA), and ethylenediaminetetraacetic acid (EDTA) were obtained from Dojindo Laboratories (Kumamoto, Japan). Other chemicals were of the best grades commercially available, and all solutions were made in deionized and distilled water.

*Synthesis and purification of recombinant HSA.* Wild-type HSA and the H3A mutant were synthesized, using *P. pastoris* GS115 his4, and purified as previously described [9]. The mutagenic primers (sense and antisense) for making the mutant were:

5′-GCTCATCCGATGGCCACAAGAGTGAGG-3′, and 3′-CCTCA CTCTTGTGGCCATCGGATGAGC-5′.

The albumins were deionized and defatted via charcoal treatment, freeze-dried, and then stored at −20 °C until used. According to density analysis of Coomassie Brilliant Blue-stained protein bands on 12.5% SDS–PAGE, the purity of the protein samples were more than 97%.

*Preparation of ligand-HSA solutions.* First, HSA was treated with DTT as follows. HSA (300 μM) was incubated with DTT (molar ratio, protein:DTT = 1:10) for 5 min at 37 °C. After that, DTT was quickly removed by Sephadex G-25 gel filtration using 10 mM phosphate-buffered saline (pH 7.4) (PBS; $Ca^{2+}$, $Mg^{2+}$ free). Stock solutions of 20 mM OA and 20 mM progesterone were made in methanol-$H_2O$ (1:1, v/v) and ethanol-$H_2O$ (1:1, v/v), respectively, whereas 20 mM BR was made in 0.1 N NaOH and protected against light. Later, these stock-solutions were diluted with PBS. Other ligands were directly dissolved in PBS. In all cases, the resulting solutions were mixed with PBS containing HSA. The ligand–protein solutions, except for those having $CuSO_4$, were incubated for 30 min at 37 °C in the dark. Freshly prepared $CuSO_4$-HSA solutions were also incubated for 30 min in the dark but at 4 °C, because the SH-group of HSA easily undergoes oxidation in the presence of $Cu^{2+}$. To remove free ligands, mixtures were applied to a Sephadex G-25 column, quickly eluted with PBS and concentrated by ultrafiltration. The protein content of all protein preparations used in this study was determined by the Bradford assay.

*Accessibility of Cys-34.* In reduced HSA this was estimated with Ellman's reagent, DTNB. Briefly, the accessibility was evaluated as $A_5/A_{60}$, where $A_5$ and $A_{60}$ is the sample absorbance at 405 nm after 5 min and 60 min (maximal absorbancy), respectively, of incubation with DTNB [12].

*S-Nitrosylation of HSA in cell-free reaction systems.* SNO-HSA was prepared with protection against light and according to previous reports [13,14]. HSA (100 μM) with and without ligand was incubated with GS-NO or NOC-7 as NO donor (molar ratio, protein:NO donor = 1:5) in PBS for 10 min at 37 °C. To remove NO donors, S-nitrosylated products were applied to a Sephadex G-25 column, eluted with PBS containing 0.5 mM DTPA, and concentrated by ultrafiltration. These samples were stored at −80 °C until analyzed.

*Determination of S-nitrosylation efficiency.* The amounts of the S-nitroso moiety of SNO-HSA were quantified by HPLC coupled with a flow-reactor system, as previously reported [13,15]. The HPLC column was a gel filtration column for S-nitrosylated proteins (φ8 × 300 mm), Diol-120, YMC, Kyoto, Japan. Briefly, the eluate from the HPLC column was mixed with a $HgCl_2$ solution to decompose S-nitrosylated compounds to yield $NO_2^-$ (via $NO^+$). The $NO_2^-$ generated was then detected after reaction with Griess reagent in the flow-reactor system.

*SNO-HSA production by cells in culture.* RAW264.7 cells were cultured in 24-well plates (16-mm diameter; Falcon, Lincoln Park, NJ) with Dulbecco's modified Eagle's medium supplemented with 10% fetal bovine serum and nonessential amino acids (Life Technologies, Inc.). Cells at saturation density ($1 \times 10^6$ cells/well) were stimulated with interferon-γ (Genzyme, Cambridge, MA) at 100 U/ml and lipopolysaccharide (*Escherichia coli* 026B; Difco) at 10 μg/ml for 12 h at 37 °C in a $CO_2$ incubator (5% $CO_2$, 95% air (v/v)). The culture medium was removed, and the cells were washed three times with PBS (pH 7.4). Cells were further incubated in the $CO_2$ incubator at 37 °C with 200 μl of PBS containing 0.5 mM L-arginine and 100 μM HSA alone or with bound ligand. After incubation for 10 min, the reaction medium was mixed with 1/10 volume of 5 mM DTPA dissolved in PBS (pH 7.4), followed by centrifugation at 10,000*g* for 10 min at 4 °C. The resultant supernatants were stored at −80 °C until applied to the HPLC-flow reactor system.

*Statistical analysis.* The statistical significance of collected data was evaluated using the ANOVA analysis followed by Newman–Keuls method for more than 2 means. Differences between groups were evaluated by the Student's *t* test. $P < 0.05$ was regarded as statistically significant.

## Results and discussion

### *S-Nitrosylation of mercaptalbumin with bound ligands*

HSA purified from serum has bound endogenous ligands, in particular fatty acids, and perhaps also exogenous ligands. Any effect of these ligands on the S-nitrosylation of HSA was examined by incubating non-defatted and charcoal-treated albumin with GS-NO. The S-nitroso moiety of the former preparation was $0.41 \pm 0.02$ ($n = 4$), whereas that of the latter was only $0.19 \pm 0.01$ ($P < 0.01$). Thus, the presence of ligands greatly enhanced the efficiency of S-nitrosylation. In order to identify ligands of importance for S-nitrosylation, individual ligands were added to HSA, which had been delipidated by charcoal and dialyzed extensively against deionized water. In these experiments, two kinds of S-nitrosylating agents were used, namely GS-NO which S-transnitrosylates via $NO^+$, and NOC-7 which S-nitrosylates mainly via NO and $N_2O_3$. The results obtained with equimolar amounts of protein and ligand are given in Figs. 1A and 2A. It can be seen that OA and BR enhances the efficiency of GS-NO, but not that of NOC-7, whereas $Cu^{2+}$ increases the S-nitrosylation by NOC-7 but not that caused by GS-NO. In contrast, no significant effect was observed when adding L-tryptophan,

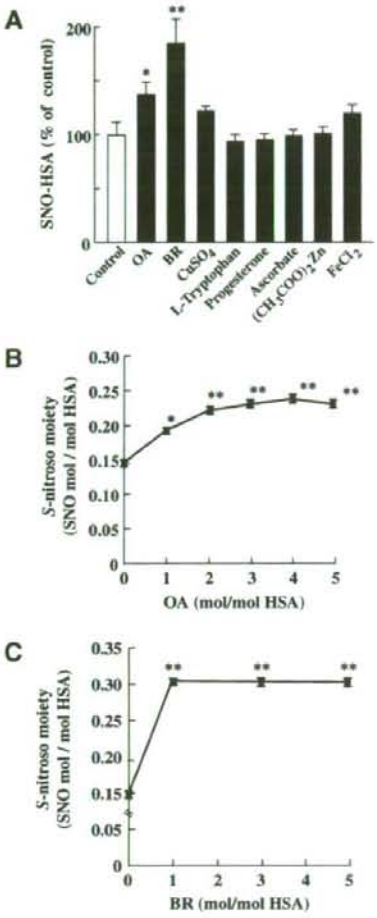


Fig. 1. Effect of ligand binding on S-nitrosylation of HSA by GS-NO. (A) 100 μM DTT-treated HSA was incubated with 100 μM of different ligands. (B) DTT-treated HSA was incubated with different molar ratios of OA. (C) DTT-treated HSA was incubated with different molar ratios of BR. In all cases, the GS-NO concentration was 500 μM. Data are expressed as means ± SEM ($n = 4$–6). $^{*}P < 0.05$, $^{**}P < 0.01$, as compared with control.

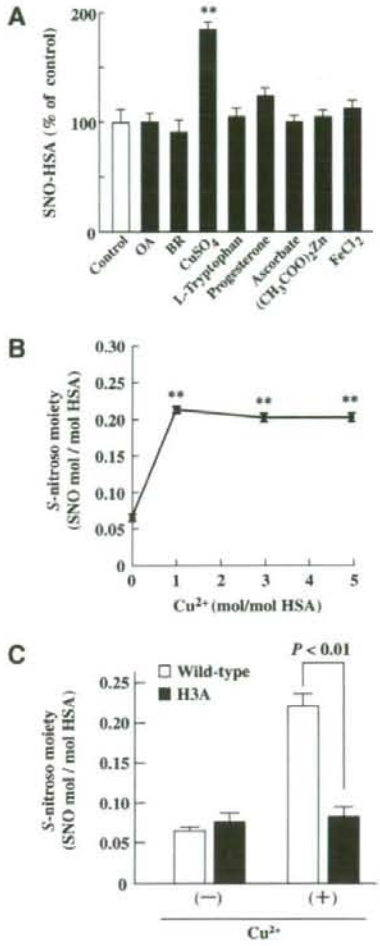


Fig. 2. Effect of ligand binding on S-nitrosylation of HSA by NOC-7. (A) Hundred micromolars of DTT-treated HSA was incubated with 100 μM of different ligands. (B) DTT-treated HSA was incubated with different molar ratios of $Cu^{2+}$. (C) Wild-type HSA and the H3A mutant, without or with $Cu^{2+}$, were S-nitrosylated by NOC-7. In all cases, the NOC-7 concentration was 500 μM. Data are expressed as means ± SEM ($n = 4$–6). $^{**}P < 0.01$, as compared with control.

progesterone, ascorbate, $(CH_3COO)_2Zn$ or $FeCl_2$. In the following, we have studied in more detail the positive effects of OA, BR and $Cu^{2+}$, which bind to different high-affinity sites of HSA [10,16] (Fig. 3).

Fig. 1B shows an increasing effect of OA on S-nitrosylation of HSA by GS-NO. The increment is dose-dependent until a OA:HSA molar ratio of 3; increasing the molar ratio further to 4 or 5 did not result in additional S-nitrosylation. Because OA does not bind to Cys-34 (Fig. 3), the effect observed could be due to binding-induced conformational changes of HSA making Cys-34 more accessible to GS-NO [12,17]. Actually, the data given in Table 1 propose such a mechanism, because OA binding results in an almost linear increment in binding of the test-compound DTNB to Cys-34.

The effect of BR binding on S-nitrosylation by GS-NO was also studied at different molar ratios of ligand to protein (Fig. 1C). Without BR the amount of S-nitroso moieties was $0.15 \pm 0.02$ ($n = 3$), and with BR it was approximately 0.30 ($P < 0.01$). The latter value was obtained, whether the BR:HSA molar ratio was 1, 3 or 5. Thus, only high-affinity BR binding increases S-nitrosylation. Because this kind of binding takes place to another region of HSA than that housing Cys-34 (Fig. 3) the improving effect must be the result of conformational

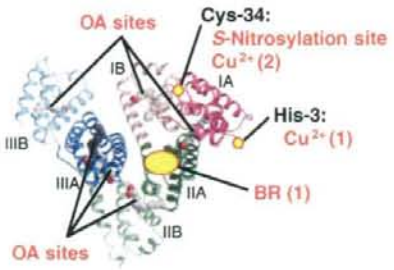


Fig. 3. Crystal structure of HSA showing locations of OA binding sites, high-affinity binding sites for BR (BR(1)) and $Cu^{2+}$ ($Cu^{2+}(1)$) and Cys-34 which also is the site for secondary $Cu^{2+}$ binding ($Cu^{2+}(2)$). The subdivision of HSA into domains (I-III) and subdomains (A and B) is indicated. The structure was simulated on the basis of X-ray crystallographic data for HSA-OA (PDB ID code 1gni) and modified with the use of Rasmol (downloaded from http://www.openrasmol.org).

Table 1
Effect of binding on the accessibility of Cys-34

| Ligand/HSA | 0 | 1 | 3 | 5 |
|---|---|---|---|---|
| OA | $0.17 \pm 0.01$ | $0.22 \pm 0.02^{*}$ | $0.67 \pm 0.03^{**}$ | $0.84 \pm 0.04^{**}$ |
| BR | $0.17 \pm 0.02$ | N.D. | N.D. | N.D. |
| $Cu^{2+}$ | $0.17 \pm 0.02$ | $0.18 \pm 0.03$ | $0.20 \pm 0.04$ | $0.19 \pm 0.04$ |

The accessibility was evaluated as A5/A60, where A5 and A60 is the sample absorbance at 405 nm after 5 min and 60 min (maximal absorbancy), respectively, of incubation with DTNB [12]. Results are given as means ± SEM ($n = 5$). N.D., not determined. $^{*}P < 0.05$, $^{**}P < 0.01$, as compared with Ligand/HSA = 0.

changes in the protein related to accommodation of the large BR molecule. That such conformational changes take place has previously been detected by techniques such as fluorescence spectroscopy [10]. By contrast to GS-NO, high-affinity binding of BR does not influence S-nitrosylation by NOC-7 (Fig. 2A). For testing whether this lack of effect could be caused by an interaction between NO and HSA-bound BR, we performed spectrophotometric experiments. These experiments showed that exposure of HSA-BR to NOC-7, but not to GS-NO, results in a fast decrease of the absorbancy at 470 nm (representing $\lambda_{max}$ for HSA-BR) and a concomitant and pronounced increase at 650 nm (representing $\lambda_{max}$ for HSA-biliverdin) (data not shown). Therefore, the following reaction seems to have taken place: ($^{34}$Cys-SH)-HSA-BR + ·NO → ($^{34}$Cys-SH)-HSA-BV + $NO_2^-$. Thus, the lack of effect of BR is due to a conversion to biliverdin (BV), and neither that ligand nor the $NO_2^-$ formed can improve S-nitrosylation.

In contrast to the S-nitrosylating effect of GS-NO, the effect of NOC-7 was significantly increased by the presence of $Cu^{2+}$ (Fig. 2A). The increasing effect was the same, whether the molar ratio of $Cu^{2+}$ to protein was 1:1, 3:1 or 5:1 (Fig. 2B). $Cu^{2+}$ binds with a very high affinity to a specific site in the N-terminal region of HSA, and His-3 is an essential element of that site [10]. In order to test whether high-affinity binding of $Cu^{2+}$, which takes place at a distance from Cys-34 (Fig. 3), is responsible for the improving effect of NOC-7, or whether the effect is caused by other means, e.g. secondary binding, we mutated His-3 for an alanine. The results of Fig. 2C show that the positive effect of $Cu^{2+}$ disappears when mutating His-3. This finding strongly proposes high-affinity binding as the reason for the improving effect of $Cu^{2+}$ on the S-nitrosylation by NOC-7. The positive effect of high-affinity $Cu^{2+}$ binding is most probably caused by conformational changes induced in the HSA molecule, which render the SH-group of Cys-34 more reactive. Such a mechanism also seems to be supported by the results of Zhang and Wilcox [18]. These authors, using isothermal titration calorimetry and different spectroscopic techniques, found evidence for an interaction between the first $Cu^{2+}$ binding site and Cys-34 in bovine serum albumin. However, these conformational changes are different from those caused by OA, because in contrast to OA binding of $Cu^{2+}$ does not affect the accessibility of Cys-34 (Table 1). In contrast to the present findings Stubauer et al. [19] found no effect of high-affinity bound $Cu^{2+}$ on RS-NO formation. RS-NO formation was only initiated, when that binding site was saturated, and the authors proposed S-nitrosylation of Cys-34 when also $Cu^{2+}$ binds with a low affinity to the same residue. However, they used bovine serum albumin and NO gas in their studies.

### *S-Nitrosylation of mercaptalbumin-ligand complexes by NOC-7 and RAW264.7 cells*

For studying S-nitrosylation of HSA in a biological system, we investigated the process caused by the murine macrophage cell line RAW264.7 (Fig. 4). The cell line had been activated by interferon-γ and lipopolysaccharide for expressing the inducible NO synthase. Binding of OA or BR does not affect S-nitrosylation of HSA by the cells. By contrast, $Cu^{2+}$ binding facilitates S-nitrosylation (Fig. 4B). Fig. 4C shows that binding of $Cu^{2+}$, but not binding of OA or BR, decreases significantly the production of $NO_2^-$. These results propose that the formation of SNO-HSA by the cell line takes place via NO. This proposal was supported by findings showing that the effects of GS-NO in a similar experiment were different from those of NOC-7 and the RAW cells (data not shown).

### *Concluding remarks*

Normally, the molar ratio of endogenous fatty acids to HSA is about 1.5 or lower [10], and those of BR and $Cu^{2+}$ are below unity. Strenuous exercise or other adrenergic stimulation can rise the molar ratio for fatty acids to about 4 [10]. The molar ratios of all three ligands can be elevated in pathological conditions, e.g., metabolic syndrome, Type II (non-insulin-dependent) diabetes (fatty acids), increased catabolism of hemoglobin or hepatic

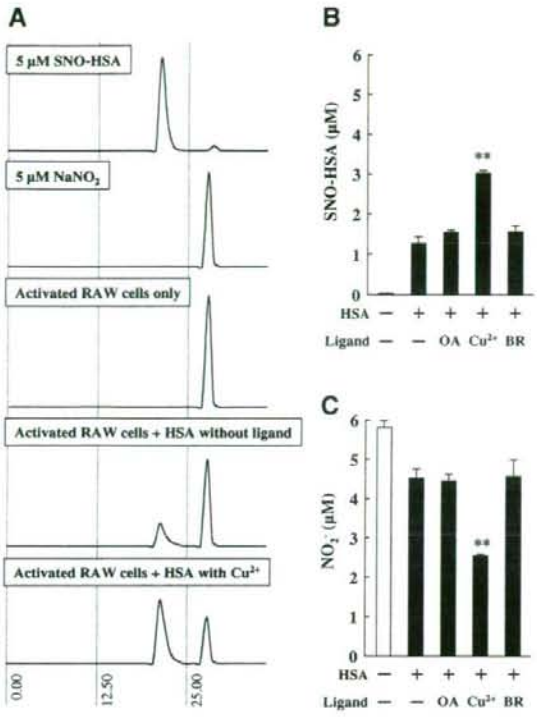


Fig. 4. Effect of high-affinity binding of OA, $Cu^{2+}$ and BR on S-nitrosylation of HSA by activated RAW264.7 cells. (A) Elution profiles for the standard solutions (5 μM SNO-HSA and 5 μM $NaNO_2$) and for different cell media made by the HPLC-flow reactor system. The retention time for SNO-HSA and $NO_2^-$ is about 21 and 27 min, respectively. (B) Production of SNO-HSA from HSA with and without bound ligand. (C) Production of $NO_2^-$ in the presence of HSA with and without bound ligand. Data are expressed as means ± SEM ($n = 4$–6). $^{**}P < 0.01$, as compared with HSA without bound ligand.

disorders (BR) and Wilson's disease ($Cu^{2+}$). Thus, several physiological, clinical and pathological situations can affect the concentration of the quantitatively important SNO-HSA via modified high-affinity binding of OA, BR or $Cu^{2+}$.

In addition to HSA, other proteins possessing a free cysteine residue can be targets for S-nitrosylation, e.g. $\alpha_1$-protease inhibitor [20]. Many of these proteins also bind ligand(s) the amounts of which can change in different biological or pathological conditions. Therefore, the present observations made with HSA could be general effects also applying to other proteins binding ligands and NO.

## Acknowledgments

We are grateful to Dr. Ayaka Suenaga and Dr. Yasunori Iwao at the Graduate School of Pharmaceutical Sciences, Kumamoto University for helpful discussions. Thanks are also due to members of the Gene Technology Center in Kumamoto University for their important contributions to the experiments.

## References

[1] L.J. Ignarro, P.J. Kadowitz, W.H. Baricos, Evidence that regulation of hepatic guanylate cyclase activity involves interactions between catalytic site -SH groups and both substrate and activator, Arch. Biochem. Biophys. 208 (1981) 75–86.
[2] L.J. Ignarro, H. Lippton, J.C. Edwards, W.H. Baricos, A.L. Hyman, P.J. Kadowitz, C.A. Gruetter, Mechanism of vascular smooth muscle relaxation by organic nitrates, nitrites, nitroprusside and nitric oxide: evidence for the involvement of S-nitrosothiols as active intermediates, J. Pharmacol. Exp. Ther. 218 (1981) 739–749.
[3] L.J. Ignarro, B.K. Barry, D.Y. Gruetter, J.C. Edwards, E.H. Ohlstein, C.A. Gruetter, W.H. Baricos, Guanylate cyclase activation of nitroprusside and nitrosoguanidine is related to formation of S-nitrosothiol intermediates, Biochem. Biophys. Res. Commun. 94 (1980) 93–100.
[4] N. Hogg, Biological chemistry and clinical potential of S-nitrosothiols, Free. Radic. Biol. Med. 28 (2000) 1478–1486.
[5] M.W. Foster, T.J. McMahon, J.S. Stamler, S-Nitrosylation in health and disease, Trends Mol. Med. 9 (2003) 160–168.
[6] J.S. Stamler, D.I. Simon, J.A. Osborne, M.E. Mullins, O. Jaraki, T. Michel, D.J. Singel, J. Loscalzo, S-Nitrosylation of proteins with nitric oxide: synthesis and characterization of biologically active compounds, Proc. Natl. Acad. Sci. USA 89 (1992) 444–448.
[7] S. Hallstrom, H. Gasser, C. Neumayer, A. Fugl, J. Nanobashvili, A. Jakubowski, I. Huk, G. Schlag, T. Malinski, S-Nitroso human serum albumin treatment reduces ischemia/reperfusion injury in skeletal muscle via nitric oxide release, Circulation 105 (2002) 3032–3038.
[8] M. Dworschak, M. Franz, S. Hallstrom, S. Semsroth, H. Gasser, M. Haisjackl, B.K. Podesser, T. Malinski, S-Nitroso human serum albumin improves oxygen metabolism during reperfusion after severe myocardial ischemia, Pharmacology 72 (2004) 106–112.
[9] Y. Ishima, T. Sawa, U. Kragh-Hansen, Y. Miyamoto, S. Matsushita, T. Akaike, M. Otagiri, S-Nitrosylation of human variant albumin Liprizzi (R410C) confers potent antibacterial and cytoprotective properties, J. Pharmacol. Exp. Ther. 320 (2007) 969–977.
[10] T. Peters Jr., All About Albumin: Biochemistry, Genetics, and Medical Applications, Academic Press, San Diego, 1996.
[11] R.F. Chen, Removal of fatty acids from serum albumin by charcoal treatment, J. Biol. Chem. 242 (1967) 173–181.
[12] Y.A. Gryzunov, A. Arroyo, J.L. Vigne, Q. Zhao, V.A. Tyurin, C.A. Hubel, R.E. Gandley, Y.A. Vladimirov, R.N. Taylor, V.E. Kagan, Binding of fatty acids facilitates oxidation of cysteine-34 and converts copper-albumin complexes from antioxidants to prooxidants, Arch. Biochem. Biophys. 413 (2003) 53–66.
[13] T. Akaike, K. Inoue, T. Okamoto, H. Nishino, M. Otagiri, S. Fujii, H. Maeda, Nanomolar quantification and identification of various nitrosothiols by high performance liquid chromatography coupled with flow reactors of metals and Griess reagent, J. Biochem. (Tokyo) 122 (1997) 459–466.
[14] N. Ikebe, T. Akaike, Y. Miyamoto, K. Hayashida, J. Yoshitake, M. Ogawa, H. Maeda, Protective effect of S-nitrosylated alpha(1)-protease inhibitor on hepatic ischemia-reperfusion injury, J. Pharmacol. Exp. Ther. 295 (2000) 904–911.
[15] K. Inoue, T. Akaike, Y. Miyamoto, T. Okamoto, T. Sawa, M. Otagiri, S. Suzuki, T. Yoshimura, H. Maeda, Nitrosothiol formation catalyzed by ceruloplasmin. Implication for cytoprotective mechanism in vivo, J. Biol. Chem. 274 (1999) 27069–27075.
[16] U. Kragh-Hansen, Molecular aspects of ligand binding to serum albumin, Pharmacol. Rev. 33 (1981) 17–53.
[17] I. Petitpas, T. Grune, A.A. Bhattacharya, S. Curry, Crystal structures of human serum albumin complexed with monounsaturated and polyunsaturated fatty acids, J. Mol. Biol. 314 (2001) 955–960.

[18] Y. Zhang, D.E. Wilcox, Thermodynamic and spectroscopic study of Cu(II) and Ni(II) binding to bovine serum albumin, J. Biol. Inorg. Chem. 7 (2002) 327–337.
[19] G. Stubauer, A. Giuffre, P. Sarti, Mechanism of S-nitrosothiol formation and degradation mediated by copper ions, J. Biol. Chem. 274 (1999) 28128–28133.
[20] Y. Miyamoto, T. Akaike, M.S. Alam, K. Inoue, T. Hamamoto, N. Ikebe, J. Yoshitake, T. Okamoto, H. Maeda, Novel functions of human alpha(1)-protease inhibitor after S-nitrosylation: inhibition of cysteine protease and antibacterial activity, Biochem. Biophys. Res. Commun. 267 (2000) 918–923.

0022-3565/08/3251-69–76$20.00
THE JOURNAL OF PHARMACOLOGY AND EXPERIMENTAL THERAPEUTICS
Copyright © 2008 by The American Society for Pharmacology and Experimental Therapeutics
JPET 325:69–76, 2008

Vol. 325, No. 1
132100/3322647
*Printed in U.S.A.*

# Design and Evaluation of *S*-Nitrosylated Human Serum Albumin as a Novel Anticancer Drug

Naohisa Katayama, Keisuke Nakajou, Hisakazu Komori, Kunitoshi Uchida, Jun-ichi Yokoe, Norikiyo Yasui, Hisashi Yamamoto, Toshiya Kai, Makoto Sato, Takenobu Nakagawa, Motohiro Takeya, Toru Maruyama, and Masaki Otagiri

*Departments of Biopharmaceutics (N.K., H.K., T.K., M.O.) and Clinical Pharmaceutics (T.M.), Graduate School of Pharmaceutical Sciences, and Department of Cell Pathology (T.N., M.T.), Graduate School of Medical Sciences, Kumamoto University, Kumamoto, Japan; and Pharmaceutical Research Center, Nipro Corporation, Shiga, Japan (N.K., K.N., K.U., J.-i.Y., N.Y., H.Y., T.K., M.S.)*

Received September 26, 2007; accepted January 23, 2008

**ABSTRACT**

In recent studies, the cytotoxic activity of NO has been investigated for its potential use in anticancer therapies. Nitrosated human serum albumin (NO-HSA) may act as a reservoir of NO in vivo. However, there are no published reports regarding the effects of NO-HSA on cancer. Therefore, the present study investigated the antitumor activity of NO-HSA. NO-HSA was prepared by incubating HSA, which had been sulfhydrylated using iminothiolane, with isopentyl nitrite (6.64 mol NO/mol HSA). Antitumor activity was examined in vitro using murine colon 26 carcinoma (C26) cells and in vivo using C26 tumor-bearing mice. Exposure to NO-HSA increased the production of reactive oxygen species in C26 cells. Flow cytometric analysis using rhodamine 123 showed that NO-HSA caused mitochondrial depolarization. Activation of caspase-3 and DNA fragmentation were observed in C26 cells after incubation with 100 μM NO-HSA for 24 h, and NO-HSA inhibited the growth of C26 cells in a concentration-dependent manner. The growth of C26 tumors in mice was significantly inhibited by administration of NO-HSA compared with saline and HSA treatment. Immunohistochemical analysis of tumor tissues demonstrated an increase in terminal deoxynucleotidyl transferase dUTP nick-end labeling-positive cells in NO-HSA-treated mice, suggesting that inhibition of tumor growth by NO-HSA was mediated through induction of apoptosis. Biochemical parameters (such as serum creatinine, blood urea nitrogen, aspartate aminotransferase, and alanine aminotransferase) showed no significant differences among the three treatment groups, indicating that NO-HSA did not cause hepatic or renal damage. These results suggest that NO-HSA has the potential for chemopreventive and/or chemotherapeutic activity with few side effects.

Although cancer primarily arises from disorders of cell proliferation, it also may arise from disruptions in programmed cell death signaling pathways, resulting in decreased apoptosis of cancerous cells (Okada and Mak, 2004). Therefore, induction of apoptosis in neoplastic cells is a very effective therapy for tumor eradication (Meng et al., 2006). However, this type of chemotherapy often has negative side effects, such as transient cell cycle arrest, senescence, and autophagy. Drug delivery systems that facilitate selective apoptosis of neoplastic cells have been suggested as a way of overcoming this problem (Kaufmann and Gores, 2000; Kondo et al., 2005).

NO is a unique diffusible molecular messenger that occupies a central role in mammalian pathophysiology (Brune et al., 1998). Its multiple actions include vascular smooth muscle relaxation (Moncada et al., 1986; Ignarro, 1989), inhibition of platelet aggregation (Azuma et al., 1986), effects on neurotransmission (Garthwaite, 1991), and regulation of immune function (Marletta et al., 1988). Alternatively, under some circumstances, NO is cytotoxic (Laval and Wink, 1994). NO causes cellular iron losses and inhibits DNA synthesis, mitochondrial respiration, and aconitase activity in L10 hepatoma cells (Hibbs et al., 1988). In addition, NO reacts with

Article, publication date, and citation information can be found at http://jpet.aspetjournals.org.
doi:10.1124/jpet.107.132100.

**ABBREVIATIONS:** NSAID, nonsteroidal anti-inflammatory drug; ASA, aspirin; HSA, human serum albumin; DTPA, diethylenetriaminepentaacetic acid; HBSS, Hanks' balanced salt solution; rHSA, recombinant human serum albumin; PAGE, polyacrylamide gel electrophoresis; C26, murine colon 26 carcinoma; ROS, reactive oxygen species; PBS, phosphate-buffered saline; CM-$H_2$DCFDA, 5-(and-6)-chloromethyl-2′,7′-dichlorodihydrofluorescein diacetate, acetyl ester; TUNEL, terminal deoxynucleotidyl transferase dUTP nick-end labeling; Cr, serum creatinine; BUN, blood urea nitrogen; ALT, alanine aminotransferase; AST, aspartate aminotransferase; ALP, alkaline phosphatase; BSA, bovine serum albumin; GSNO, *S*-nitrosoglutathione; R410C, genetic variant of human serum albumin mutated at position 410.

superoxide anion (which is produced by activated macrophages and other cells), to form peroxynitrite. This by-product of NO is a potent chemical oxidant, which alters protein function and damages DNA (Beckman and Crow, 1993). These effects are part of the nonspecific host defense, which facilitates killing of tumor cells and intracellular pathogens. In addition, the cytotoxicity arising from long-lasting NO generation has been attributed to induction of apoptosis (Brune et al., 1998).

In recent studies, the cytotoxic activity of NO has been studied to assess its therapeutic potential in cancer treatment. NO-donating nonsteroidal anti-inflammatory drugs (NSAIDs), especially NO-aspirin (NO-ASA), have been investigated as promising chemopreventive agents (Williams et al., 2001; Kashfi et al., 2002; Fabbri et al., 2005). NO-ASA consists of traditional ASA to which an NO-releasing moiety is bound via a spacer. This agent induces oxidative stress by increasing intracellular peroxide and $O_2^{\cdot}$, thereby inducing apoptosis via activation of the intrinsic apoptosis pathway (Gao et al., 2005). JS-K is a prodrug designed to release NO after reacting with glutathione transferase, which induces double-stranded DNA breaks, activates DNA damage response pathways, and induces apoptosis in human multiple myeloma cells both in vitro and in vivo (Kiziltepe et al., 2007).

Human serum albumin (HSA) is an abundant circulating protein, and the nitrosated form serves as a reservoir of NO (Stamler et al., 1992). Therefore, NO-HSA is an NO donor that is currently being investigated for its potential therapeutic applications. For example, administration of NO-HSA to animals with ischemia-reperfusion injury minimizes the tissue damage that occurs after reperfusion (Semsroth et al., 2005). In a balloon-injured rabbit femoral artery model, locally delivered NO-HSA preferentially binds to sites of vessel injury and inhibits both platelet accumulation and the subsequent development of neointimal hyperplasia (Marks et al., 1995). NO-HSA also shows potent antibacterial activity and inhibits the proliferation of cultured human vascular smooth muscle cells (Ishima et al., 2007). However, there are no reports describing the effects of NO-HSA on cancer.

Accordingly, the present study evaluated the antitumor activity of NO bound to HSA (NO-HSA) via an *S*-nitrosothiol linkage using iminothiolane as a spacer. The molecular events related to induction of apoptosis by NO-HSA were studied in vitro, and the antitumor activity of NO-HSA was studied in vivo using a murine model of C26 colon carcinoma.

## Materials and Methods

**Chemicals.** Traut's reagent (2-imminothiolane) was purchased from Pierce Chemical (Rockford, IL). Isopentyl nitrite, diethylenetriaminepentaacetic acid (DTPA), and Cell Counting Kit-8 (WST-8) were purchased from Wako Pure Chemicals (Osaka, Japan). RPMI 1640 medium, Hanks' balanced salt solution (HBSS), and RNase A were obtained from Sigma-Aldrich (St. Louis, MO). Proteinase K was obtained from Roche Applied Science (Indianapolis, IN). All other reagents used were of the highest grade available from commercial sources.

**Expression and Purification of Recombinant HSA.** rHSA was produced using a yeast expression system as described previously (Matsushita et al., 2004). In brief, for constructing the HSA expression vector pPIC9-HSA, native HSA coding region was incorporated into the methanol-inducible pPIC9 vector (Invitrogen, Carlsbad, CA). The resulting vector was introduced into the yeast species *Pichia pastoris* (strain GS115) to express rHSA. Secreted rHSA was isolated from the growth medium by a combination of precipitation with 60% (w/v) $(NH_4)_2SO_4$ and purification on a Blue Sepharose CL-6B column (GE Healthcare, Little Chalfont, Buckinghamshire, UK) followed by Phenyl HP column (GE Healthcare). Isolated protein was defatted by using the charcoal procedure described by Chen (1967), deionized, freeze-dried, and then stored at −20°C until use. The resulting rHSA (treated with dithiothreitol) exhibited a single band on SDS-PAGE. Density analysis of protein bands stained with Coomassie Brilliant Blue showed that its purity was more than 97%.

**Synthesis of NO-HSA.** Terminal sulfhydryl groups were added to the HSA molecule by incubating 0.15 mM rHSA with 3 mM Traut's reagent in 100 mM potassium phosphate buffer containing 0.5 mM DTPA, pH 7.8, for 1 h at room temperature. The resultant modified rHSA then was *S*-nitrosylated by 3-h incubation with 15 mM isopentyl nitrite at room temperature (Fig. 1). The resulting NO-HSA was concentrated, exchanged with saline using a PelliconXL filtration device (Millipore Corporation, Billerica, MA), and the final concentration adjusted to 2 mM NO-HSA. The sample was stored at −80°C until use.

**Determination of S-Nitrosylation Efficiency.** The amount of the *S*-nitroso moieties of NO-HSA was quantified using a 96-well plate. First, 20-μl aliquots of NO-HSA solution and $NaNO_2$ (standard) were incubated with 0.2 ml of 10 mM sodium acetate buffer, pH 5.5, containing 100 mM NaCl, 0.5 mM DTPA, 0.015% *N*-1-naphthylsthylene-diamide and 0.15% sulfanilamide with or without 0.09 mM $HgCl_2$, for 30 min at room temperature. Then, the absorbance was measured at 540 nm. The number of moles of NO per mole of HSA was obtained by subtracting the values in the absence of $HgCl_2$ from values in the presence of $HgCl_2$; the value thus obtained, was 6.64 ± 0.54 mol NO/mol HSA.

**Cellular Experiments with C26 Cells.** C26 cells, which were donated by the Institute of Development, Aging and Cancer, at Tohoku University (Sendai, Miyagi, Japan), were cultured at 37°C in RPMI 1640 medium containing 10% fetal calf serum, 100 U/ml penicillin, and 10 μg/ml streptomycin (medium A). Trypsin (0.25%) EDTA solution was used to detach the cells from the culture flask for plating and passing the cells. All cell culture experiments were performed at 37°C in a humidified atmosphere of 5% $CO_2$ in air.

For detection of reactive oxygen species (ROS), C26 cells ($1.0 \times 10^4$ cells/well) were cultured in 96-well plates in medium A for 12 h, they were washed twice with PBS, and then they were incubated for an additional 30 min in HBSS containing 5 μM 5-(and-6)-chloromethyl-2′,7′-dichlorodihydrofluorescein diacetate, acetyl ester (CM-$H_2$DCFDA) (Invitrogen, Carlsbad, CA). After washing twice with HBSS, the cells were cultured in HBSS containing 5% fetal calf serum for 15 min followed by the addition of PBS, 50 μM HSA, or 50 μM NO-HSA. After incubation, fluorescence was measured using a plate reader (excitation wavelength, 485 nm; emission wavelength, 535 nm). The change in fluorescence was calculated by subtracting the fluorescence at 0 h from the fluorescence measured at the indicated times. The fluorescence intensities of cells incubated with PBS, 50 μM HSA, and 50 μM NO-HSA at 0 h were 201.3, 166.1, and 181.3, respectively.

Changes in the mitochondrial membrane potential of C26 cells

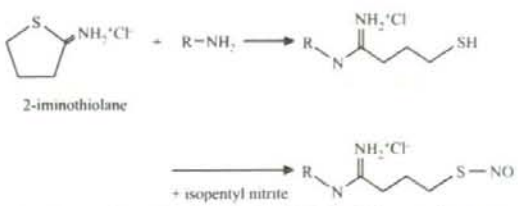


**Fig. 1.** The scheme for the reaction of 2-iminothiolane with primary amines followed by *S*-nitrosylation.

were monitored using flow cytometric analysis with rhodamine 123 staining. C26 cells ($1.0 \times 10^6$ cells/well) were cultured in six-well plates for 12 h, washed twice with PBS, and incubated with PBS and either 100 $\mu$M HSA or various concentrations of NO-HSA in medium A for 24 h. The cells were then trypsinized, washed twice with PBS, and incubated for 15 min with 5 $\mu$g/ml rhodamine 123. The mean fluorescence intensity of rhodamine 123 in the cells was measured using a flow cytometer (FACSCalibur; BD Biosciences, Franklin Lakes, NJ).

For the determination of caspase-3 activity, cells were cultured to confluence in six-well plates, washed twice with PBS, and incubated with medium A containing 100 $\mu$M HSA or various concentrations of NO-HSA. Cells were incubated for 24 h, trypsinized, and washed with 0.2 ml of ice-cold PBS. The cell pellet was resuspended in 15 $\mu$l of cell lysis buffer, it was lysed by freeze-thawing, and then it was incubated on ice for 15 min. The cell lysates were centrifuged at 15,000 rpm for 20 min at 4°C, and the supernatant fraction was collected (cell extract). The caspase-3 activity in the cell extract was assessed using the colorimetric CaspASE Assay System (Promega, Madison, WI), according to the manufacturer's instructions.

For the detection of DNA degradation (DNA ladder), C26 cells ($1.0 \times 10^6$ cell/well) were cultured in six-well plates. Cells were cultured for 12 h, they were washed twice with PBS, and then they were incubated with PBS and either 100 $\mu$M HSA or various concentrations of NO-HSA for 24 h. The cells then were trypsinized, collected, and centrifuged at 4000 rpm for 10 min. After removing the supernatant, the cell pellet was resuspended in 0.2 ml of PBS, and then it was centrifuged at 4000 rpm for 10 min. The supernatant was again removed, and the remaining pellet was incubated in 20 $\mu$l of 10 mM Tris-HCl buffer, pH 7.8, containing 2 mM EDTA and 0.5% SDS (cell lysis buffer) for 10 min at 4°C, followed by centrifugation at 15,000 rpm for 5 min. The resulting supernatant (cell extract) was collected and incubated with 1 $\mu$l of RNase A (10 $\mu$g/ml) for 30 min at 50°C. One microliter of proteinase K (10 $\mu$g/ml) was added to the cell extract, followed by a 1-h incubation at 50°C. The resulting DNA extract was electrophoresed in a 2.0% agarose gel, followed by staining of the gel with ethidium bromide and visualization of the DNA bands using ultraviolet illumination.

The cell viability assay was performed using WST-8, which is based on the 3-(4,5-dimethylthiazol-2-yl)-2,5-diphenyltetrazolium assay. C26 cells were plated in 96-well plates at $1.0 \times 10^4$ cells/well, and they were cultured for 32 h in medium A. Then, the cells were washed twice with PBS and incubated in a total volume of 0.2 ml of medium A containing various concentrations of HSA or NO-HSA. After incubating the cultures for various lengths of time, 5 $\mu$l of WST-8 solution was added to each well, and the cells were incubated for an additional 2 h at 37°C. The number of surviving cells was determined by measuring the absorbance at 450 nm. Cell viability was calculated as the percentage of the control value (without HSA or NO-HSA) (Ishiyama et al., 1996).

**Animal Experiments.** Five-week-old male BALB/c AnNCrlCrlj mice (17–20 g) were purchased from Charles River Italica (Calco, Italy). The mice were housed in a 12-h light/dark cycle in a humidity-controlled room. Mice were acclimated for at least 5 days before being used in experiments.

For tumor induction, mice were inoculated with C26 cells ($1.0 \times 10^6$ cells/mouse) by a subcutaneous injection into the dorsal skin. Three days after inoculation, C26 carcinoma-bearing mice were randomly divided into three groups: control, HSA, and NO-HSA. The mice received a daily i.v. injection of saline, HSA (10 $\mu$mol/kg), or NO-HSA (10 $\mu$mol/kg) for 10 days from day 3 to day 12 after inoculation. Tumor volume was calculated using the formula $0.4 (a \times b^2)$, where a is the largest diameter and b is the smallest diameter of the tumor (Shimizu et al., 2005), and volume was monitored from day 7 to day 17 after inoculation. Variance in each group was evaluated using the Bartlett test, and differences in mean tumor volume were evaluated using the Tukey-Kramer test.

Some animals in each of the three treatment groups were used for immunohistochemical analysis and serum biochemistry. When the mice received five times per day from day 3 to day 7 after inoculation (the tumors in each group reached approximately 5 mm in diameter), blood samples were collected from the abdominal vena cava under diethyl ether anesthesia approximately 2 h after the daily injection, and then the mice were sacrificed.

Tumors were dissected, they were fixed immediately with 2% periodate/lysine/paraform-aldehyde fixative at 4°C for 5 h, and then they were washed with a graded series of sucrose solutions in PBS (10, 15, and 20%). After immersion in 20% sucrose in PBS to inhibit ice crystal formation, the tissues were embedded in O.C.T. compound (Sakura Fine Technochemical, Tokyo, Japan), they were frozen in liquid nitrogen, and then they were stored at −80°C. Five-micrometer tumor sections were prepared using a cryostatic microtome (HM500M; Microm, Walldorf, Germany), and they were mounted on poly-L-lysine-coated slides. The slides were stained using the TUNEL method and an in situ apoptosis detection kit (Takara-Bio Co. Ltd., Shiga, Japan). The slides were washed three times with 0.01 M phosphate buffer, pH 7.4, containing 0.9% NaCl, followed by application of methanol containing 0.3% $H_2O_2$ to inactivate endogenous peroxidase and incubation at room temperature for 30 min. The slides were washed 3 times with 0.01 M phosphate-buffered saline, and then they were incubated in 100 ml of permeabilization buffer on ice for 5 min. The slides were washed three times with 0.01 M phosphate-buffered saline, and then they were incubated with 50 ml of freshly prepared terminal deoxynucleotidyl transferase reaction mixture (5 ml of terminal deoxynucleotidyl transferase enzyme + 45 ml of Labeling Safe buffer) at 37°C for 60 min. After the slides were washed three times with 0.01 M PBS, they were incubated in 70 ml of anti-fluorescein isothiocyanate-horseradish peroxidase conjugate antibody at 37°C for 30 min. After the slides were washed three times with 0.01 M PBS, they were incubated in 3,3-diaminobenzidine-$H_2O_2$ reaction buffer at room temperature for 10 min. After the slides were washed three times with distilled water, they were stained with 3% methyl green for 10 min, dehydrated, penetrated, and sealed (Gavrieli et al., 1992). Each slide then was visualized under a light microscope (Olympus, Tokyo, Japan), at a magnification of 400×.

Serum was separated by centrifugation. Routine clinical laboratory techniques were used to determine the concentrations of total protein, serum creatinine (Cr), blood urea nitrogen (BUN), alanine aminotransferase (ALT), aspartate aminotransferase (AST), and alkaline phosphatase (ALP) in serum. Variance in each group was evaluated using the Bartlett test, and differences were evaluated using the Tukey-Kramer test.

## Results

**NO-HSA Induces Cell Death via Apoptosis in Vitro.** Apoptosis is induced by a variety of factors. Among them, it is well known that intracellular accumulation of ROS, such as $H_2O_2$, $O_2^-$, and peroxynitrite, causes apoptosis. Moreover, production of ROS also plays a major role in NO-ASA-induced apoptosis. To examine whether NO-HSA promoted ROS production in C26 cells, a fluorescent probe (CM-$H_2$DCFDA), which undergoes conversion to 2',7'-dichlorofluorescein in the presence of intracellular ROS, was used. Addition of NO-HSA to C26 cells increased the amount of ROS compared with treatment with vehicle or HSA (Fig. 2). In addition, the ROS in the C26 cell culture medium increased with time after addition of NO-HSA. This result suggests that NO-HSA promotes a signal cascade leading to apoptosis by increasing intracellular production of ROS.

To evaluate the effect of NO-HSA on mitochondrial function, C26 cells were loaded with a mitochondria-selective fluorescent cation (rhodamine 123) to monitor the mitochon-

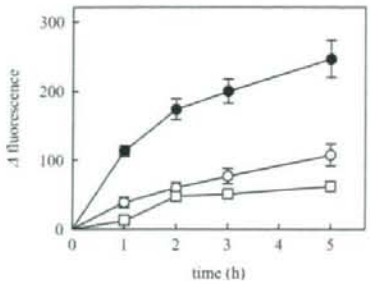


**Fig. 2.** Production of ROS in C26 cells after NO-HSA treatment. C26 cells were pretreated with CM-$H_2$DCFDA for uptake into C26 cells and hydrolysis by cellular esterase, followed by addition of either PBS (open circles), 50 $\mu$M HSA (open squares), or 50 $\mu$M NO-HSA (closed circles). Excitation of the probes was done at 485 nm, and emission was measured at 535 nm. Change in fluorescence was calculated by subtracting the fluorescence at 0 h from that at the indicated times. The fluorescence intensities of the PBS, 50 $\mu$M HSA, and 50 $\mu$M NO-HSA groups at 0 h were 201.3, 166.1, and 181.3, respectively. Results are the mean ± S.D. of three separate experiments.

drial membrane potential. Compared with vehicle, in cells treated with 50 or 100 $\mu$M NO-HSA rhodamine 123, fluorescence was decreased by 75%, whereas treatment with 25 $\mu$M NO-HSA or 100 $\mu$M HSA did not affect rhodamine 123 fluorescence compared with vehicle (Fig. 3A). These observations indicate that NO-HSA induces depolarization of the mitochondrial membrane.

Caspase-3 is a cell death protease that is involved in the downstream execution phase of apoptosis. During this phase of apoptosis, cells undergo morphological changes, such as DNA fragmentation, chromatin condensation, and formation of apoptotic bodies. Compared with the effect of vehicle, cells treated with 25 or 50 $\mu$M NO-HSA had slightly increased caspase-3 activity, and cells treated with 100 $\mu$M NO-HSA showed a larger increase in caspase-3 activity (Fig. 3B). Cells treated with HSA had the same level of caspase-3 activity as cells treated with PBS.

To further confirm that NO-HSA induced apoptosis in C26 cells, DNA fragmentation, which is a typical morphological change in the execution phase of apoptosis, was examined. DNA fragmentation was observed in C26 cells treated with 100 $\mu$M NO-HSA, but not in C26 cells treated with 25 or 50 $\mu$M NO-HSA (Fig. 3C). Neither vehicle nor 100 $\mu$M HSA induced DNA fragmentation in C26 cells (Fig. 3C). These findings suggest that NO-HSA induces apoptosis by increasing ROS production, activating caspase-3, and hyperpolarizing the mitochondrial membrane potential.

To determine the effect of NO-HSA on cell growth, the viability of C26 cells was examined after treatment with HSA or various concentrations of NO-HSA. NO-HSA inhibited growth of C26 cells in a concentration-dependent manner; cell growth was suppressed by 71, 80, and 85% after a 48-h incubation with 25, 50, and 100 $\mu$M NO-HSA, respectively (Fig. 4A). The viability of C26 cells incubated with 50 $\mu$M NO-HSA significantly decreased with increasing incubation times (Fig. 4B). NO-HSA inhibited growth to a greater extent than did HSA, which had only a weak inhibitory effect. These results suggest that NO-HSA inhibits cell growth of C26 cells by inducing apoptosis.

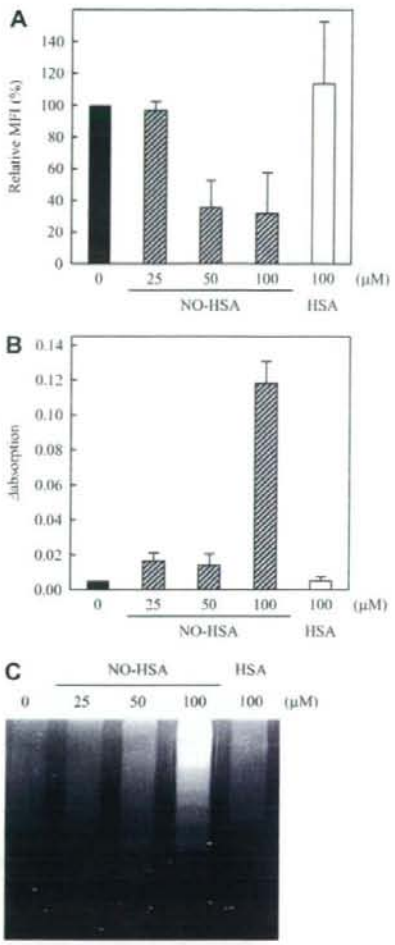


**Fig. 3.** Induction of apoptosis of C26 cells after NO-HSA treatment. A, alteration in the mitochondrial membrane potential after NO-HSA treatment. C26 cells were cultured with PBS, 100 $\mu$M HSA, or various concentrations of NO-HSA for 24 h, followed by addition of rhodamine 123. The amounts of cell-associated rhodamine 123 were determined as described under *Materials and Methods*. Results are the mean ± S.D. of three separate experiments. B, activation of caspase-3 after NO-HSA treatment. C26 cells were incubated with PBS, 100 $\mu$M HSA, or various concentrations of NO-HSA for 24 h. Caspase-3 activity was estimated by monitoring *p*-nitroaniline (absorbance at 405 nm) released from the substrate upon cleavage by caspase-3. Change in absorbance was calculated by subtracting absorbance after incubation with caspase inhibitor (*N*-benzyloxycarbonyl-Val-Ala-Asp-fluoromethylketone), from absorbance after incubation without caspase inhibitor. The absorbances among PBS-, HSA- and NO-HSA-treated cells incubated with *N*-benzyloxycarbonyl-Val-Ala-Asp-fluoromethylketone were almost identical (0.170 ± 0.17). Results are the means ± S.D. of three separate experiments. C, DNA fragmentation after NO-HSA treatment. C26 cells were incubated with PBS, 100 $\mu$M HSA or various concentrations of NO-HSA for 24 h. DNA fragmentation was detected as described under *Materials and Methods*.

**NO-HSA Exerts Antitumor Effect via the Apoptotic Pathway in Vivo.** To investigate the antitumor effect of NO-HSA in vivo, C26 tumor-bearing mice received i.v. injec-

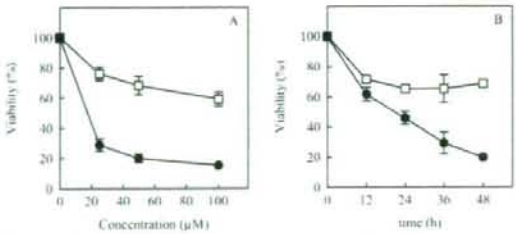


**Fig. 4.** Effect of NO-HSA on C26 cell viability. A, C26 cells were treated for 48 h with various concentrations of HSA (open squares) or NO-HSA (closed circles). B, C26 cells were incubated for the indicated times with 100 μM HSA (open squares) or 100 μM NO-HSA (closed circles). Cell viability was determined as described under *Materials and Methods*. Results are the mean ± S.D. of three separate experiments.

tions with saline, HSA, or NO-HSA. Mean tumor area increased with time in the saline-treated group. In the HSA-treated group, tumor growth was suppressed, compared with that in the control group, but the difference was not statistically significant. In contrast, tumor growth was significantly inhibited by administration of NO-HSA (Fig. 5).

To clarify whether the suppression of tumor growth by NO-HSA is mediated via apoptosis, tumor tissues from C26 tumor-bearing mice receiving injections with NO-HSA were examined using immunohistochemistry. In NO-HSA-treated mice, there were more TUNEL-positive cells than in the saline- and HSA-treated animals. In addition, the tumor tissue architecture was less defined in animals treated with NO-HSA than in the other groups, suggesting that NO-HSA induced apoptosis in C26 tumor cells and thus exerted an antitumor effect in vivo (Fig. 6).

To evaluate the side effects of NO-HSA treatment, several serum biochemical parameters were measured in tumor-bearing mice treated with saline, HSA, or NO-HSA (Table 1). There were no significant differences in total protein, Cr, BUN, AST, or ALT among the three groups, suggesting that

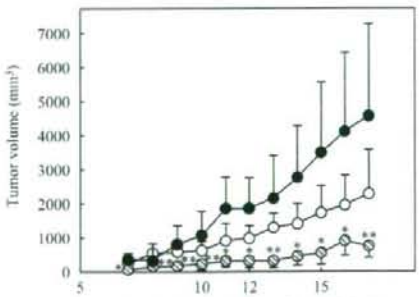


**Fig. 5.** Effect of NO-HSA on tumor growth in C26 tumor-bearing mice. C26 tumor-bearing mice were given daily i.v. injections of saline (5 ml/kg), HSA (10 μmol/5 ml/kg), or NO-HSA (10 μmol/5 ml/kg) for 10 days from day 3 to day 12 after inoculation with tumor cells. Tumor size was measured and tumor volume was calculated according to the formula: $V = 0.4a^2b$, where $a$ is the smallest, and $b$ is the largest, superficial diameter. Results are means ± S.D; $n = 10$ animals per experimental group. *, statistically significant reduction compared with saline ($P < 0.01$) or HSA ($P < 0.05$) at the corresponding time. **, statistically significant reduction compared with saline ($P < 0.01$) or HSA ($P < 0.01$) at the corresponding time.

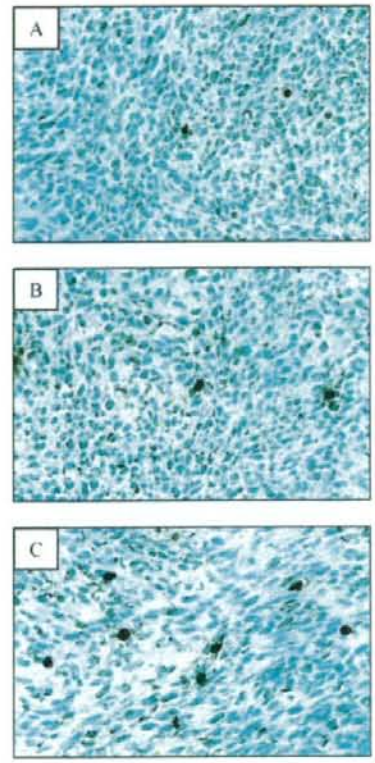


**Fig. 6.** Immunohistochemical staining of tumor tissues of C26 tumor-bearing mice receiving i.v. injections with NO-HSA using the TUNEL method. C26 tumor-bearing mice were given daily i.v. injections of saline (5 ml/kg) (A), HSA (10 μmol/5 ml/kg) (B), or NO-HSA (10 μmol/5 ml/kg) (C) for 5 days from day 3 to day 7 after inoculation with tumor cells. TUNEL staining, performed as described under *Materials and Methods*, shows apoptotic cells in the tumor tissue of mice treated with NO-HSA.

TABLE 1

Serum biochemical parameters of C26 tumor-bearing mice treated with saline, HSA, or NO-HSA

C26 tumor-bearing mice received i.v. injections five times per day with saline (5 ml/kg), HSA (10 μmol/5 ml/kg), or NO-HSA (10 μmol/5 ml/kg) from day 3 to day 7 after inoculation with tumor cells. Blood samples were collected from the abdominal vena cava under anesthesia with diethyl ether approximately 2 h after the last treatment injection, and mice were sacrificed. Serum biochemical parameters were measured using routine clinical laboratory techniques.

| Serum Biochemical Parameter | Saline | HSA | NO-HSA |
|---|---|---|---|
| Total protein (g/dl) | 5.23 ± 0.21 | 5.33 ± 0.06 | 5.55 ± 0.24 |
| Cr (mg/dl) | 0.13 ± 0.04 | 0.14 ± 0.01 | 0.16 ± 0.01 |
| BUN (mg/dl) | 15.25 ± 0.96 | 15.33 ± 1.53 | 13.75 ± 1.26 |
| AST (U/l) | 143.5 ± 62.9 | 91.7 ± 39.4 | 116.3 ± 69.1 |
| ALT (U/l) | 169.8 ± 111.6 | 110.0 ± 81.2 | 161.3 ± 126.2 |
| ALP (U/l) | 385.3 ± 18.3 | 345.3 ± 4.7* | 300.5 ± 23.0**,† |

* $P < 0.05$, saline vs. HSA.
** $P < 0.01$, saline vs. NO-HSA.
† $P < 0.05$, HSA vs. NO-HSA.

NO-HSA did not cause kidney or liver damage. However, compared with the control group, mice treated with HSA had significantly lower serum levels of ALP (345.3 ± 4.7 versus 385.3 ± 18.3 U/l). Moreover, the serum concentration of ALP

in mice treated with NO-HSA was 300.5 ± 23.0 U/l, which was significantly lower than the control ($P < 0.01$) and HSA ($P < 0.05$) groups. In general, ALP levels increase in several types of cancer, such as liver, lung, and bone cancer; thus, the present findings suggest that NO-HSA is an effective anticancer agent. The vasodilating effect of NO-HSA was also evaluated in rats after i.v. injection at a dose of 10 μmol/kg (66 μmol of NO per kg). NO-HSA induced a decrease in the mean arterial blood pressure immediately after i.v. injection and the maximum reduction effect was 32.8 ± 7.3 mm Hg. In contrast, HSA had no significant effect on the blood pressure. The fall in pressure returned to the initial levels in 30 min (data not shown).

## Discussion

There have been many trials of NO as a therapeutic agent, because of its powerful biological activity (Moncada and Higgs, 1993). However, the in vivo half-life of NO (~0.1 s) is often too short to capitalize on its potential biological actions. The half-life of NO can be prolonged by adding *S*-nitrosothiol moieties with cysteine residues of proteins. For example, nitrosated HSA seems to act as a reservoir of NO in vivo (Stamler et al., 1992). Simon et al. (1996) incubated bovine serum albumin (BSA) with 200-fold excess concentration of $NaNO_2$ under acidic condition to synthesize polynitrosylated BSA that is highly modified at the thiol group of cysteine, hydroxyl group of tyrosine and amines (38 mol NO/mol BSA). The polynitrosylated BSA has been shown to exhibit antiplatelet activity. However, polynitrosylated *S*-NO-BSA, an NO-BSA conjugate prepared with the same method except that the BSA has been reduced with dithiothreitol and it contains 19 mol of "*S*-NO" per mol of BSA, was a significantly more potent platelet inhibitor than polynitrosylated BSA described above. These findings show that nitrosylated BSA behaves as an NO donor; in particular, the poly(*S*-nitroso) derivative could be by far the most potent compound. One molecule of HSA contains 35 cysteine residues, 34 of which form 17 nonreactive disulfide bonds, and one of which (Cys-34) forms a reactive free thiol (Peters, 1985). Thus, the number of NO molecules that can be bound to HSA is limited because only one free cysteine per HSA molecule is available for conjugation. Ewing et al. increased the number of free sulfhydryl groups on BSA by reduction with dithiothreitol and thiolation with *N*-acetylhomocysteine, thereby preparing polynitrosated BSA (12–15 mol NO/mol BSA) (Ewing et al., 1997). Marks et al. (1995) produced polynitrosated BSA (5.9 mol NO/mol BSA) by adding free sulfhydryl groups to the molecule and by treating the BSA with *N*-acetylhomocysteine thiolactone. However, the polynitrosated BSAs prepared in these studies formed aggregates as a result of intermolecular disulfide formation. Aggregate formation results in molecular heterogeneity, which limits the therapeutic application of *S*-nitroso residues. In the present study, iminothiolane, which reacts with primary amines to introduce sulfhydryl groups while maintaining charge properties similar to the original amino groups, was selected as the thiolation reagent. Iminothiolane was used to produce polynitrosated HSA (NO-HSA) (6.6 mol NO/mol HSA), which did not form aggregates after nonreducing SDS-PAGE or native-PAGE (data not shown). Moreover, the far-UV CD spectra of NO-HSA were nearly identical to those of HSA (data not shown). Therefore, NO-HSA is expected to be clinically applicable as a biocompatible pharmacological agent, although further study is required to clarify other potential issues, including the antigenicity of this protein.

NO-NSAIDs have been extensively investigated as therapeutic agents for cancer due to their ability to release NO, thereby promoting apoptosis. NO-NSAIDs are categorized as organic nitrate esters, which are readily reduced to organic nitrite esters by cytosolic enzymes. Subsequently, glutathione reacts with organic nitrite esters to form GSNO, indicating that NO-NSAIDs release NO via *S*-nitrosothiol (Wong and Fukuto, 1999). Alternatively, the transfer of NO from NO-HSA to the cytosol could be inferred from a study by Ramachandran et al. (2001). They reported that NO is released from extracellular *S*-nitrosothiols by a cell surface enzyme (protein disulfide isomerase) and that it accumulates in the cell membrane where it reacts with $O_2$ to produce $N_2O_3$, which is then available for nitrosation reactions with intracellular thiols at the membrane-cytosol interface (Ramachardran et al., 2001). Therefore, it is possible that NO-HSA also releases NO by the intracellular formation of *S*-nitrosothiol, suggesting that the species of NO released within the cell by *S*-nitrosothiols, as well as the reactive substances (such as ROS) derived from the released NO, would not differ significantly between NO-NSAIDs and NO-HSA. In support of this hypothesis, NO-HSA caused depolarization of the mitochondrial membrane potential, activation of caspase-3 and DNA fragmentation in the present study, consistent with the effects of NO-NSAIDs. Additional studies are needed to determine the details of the molecular events and the systematic pathways affected by NO-HSA, but the mechanism of action should be similar to that of NO-NSAIDs. In a recent study, Gao et al. (2005) elucidated the detailed mechanism of apoptosis induced by NO-ASA. Intracellular accumulation of ROS is a key proximal event in NO-ASA-induced apoptosis, and it correlates with the effect on tumor cell growth (Gao et al., 2005). In the present study, NO-HSA induced accumulation of ROS in tumor cells, suggesting that increased ROS production may be an important proximal event leading to induction of apoptosis.

The results of the in vivo study showed that NO-HSA significantly suppressed tumor growth by inducing apoptosis, without adverse changes in serum biochemical parameters in treated mice. In a recent study, Trachootham et al. (2006), using immortalized cell lines and their oncogenic progeny transfected with *H-Ras*$^{V12}$, demonstrated that cancer cells typically produce more ROS than normal cells. Moreover, the pro-oxidant status of cancer cells increases their susceptibility to treatment with agents that cause oxidative stress, as demonstrated in a study using β-phenylethyl isothiocyanate (Trachootham et al., 2006). In addition, Feng et al. (2007) reported that cyaniding-3-rutinoside selectively induces accumulation of peroxides in HL-60 human leukemic cells, but not in normal peripheral blood mononuclear cells (Feng et al., 2007). Schumacker (2006) has proposed that ROS toxicity induced by certain chemotherapeutic agents may be an effective means of selectively eradicating malignant cells. In the present study, we presumed that although NO reacts with superoxide anion to form peroxynitrite (a potent oxidant and nitrating agent), these highly reactive oxidant species are probably produced at higher